View metadata, citation and similar papers at core.ac.uk

brought to you by CORE

provided by Helsingin yliopiston digitaalinen arkisto

Carbon isotope records of sedimentary carbonate rocks in the Pechenga belt, NW Russia: implications for the Precambrian carbon cycle

PAULA SALMINEN

ACADEMIC DISSERTATION
To be presented, with the permission of the Faculty of Sciences of the University of Helsinki, for public examination in auditorium E204, Physicum, Kumpula Campus, on June 18th, 2014, at 12 o´clock noon.

DEPARTMENT OF GEOSCIENCES AND GEOGRAPHY A25/ HELSINKI 2014

© Paula Salminen (synopsis and Paper III)
© Elsevier B.V. (Papers I and II)
Cover photo: Paula Salminen

Author´s address: Paula Salminen
Department of Geosciences and Geography
P.O.Box 64
00014 University of Helsinki
Finland
paula.salminen@helsinki.fi

Supervised by: Professor Juha Karhu
Department of Geosciences and Geography
University of Helsinki

Reviewed by: Dr. Peter Sorjonen-Ward
Geological Survey of Finland

Dr. Mark van Zuilen
Institut de Physique du Globe de Paris
Equipe Géobiosphère Actuelle et Primitive

Opponent: Assistant Professor Andrey Bekker
Department of Earth Sciences
University of California, Riverside

Department of Geosciences and Geography A
ISSN-L 1798-7911
ISSN 1798-7911
ISBN 978-952-10-9461-3 (paperback)
ISBN 978-952-10-9462-0 (PDF)
http://ethesis.helsinki.fi

Unigrafia
Helsinki 2014

Salminen P., 2014. C*arbon isotope records of sedimentary carbonate rocks in the Pechenga belt, NW Russia: implications for the Precambrian carbon cycle*. Unigrafia. Helsinki. 39 pages, 2 tables and 7 figures.

Abstract

The Archean-Paleoproterozoic transition was a time of significant global environmental events. Among the greatest of these was the rise of atmospheric oxygen, known as the Great Oxidation Event. Another major event was a global perturbation in the carbon cycle, evidenced by a global positive $\delta^{13}C$ excursion in Paleoproterozoic sedimentary carbonates, referred to as the Lomagundi-Jatuli Isotope Event (LJIE). This PhD thesis focuses on the investigation of the LJIE and its aftermath. In addition, some of the earliest travertines on Earth, associated with background stratified sedimentary carbonates, were studied in detail.

The research was based on samples of sedimentary carbonate rocks from the Pechenga Greenstone Belt, NW Russia, taken from three drillcores intersecting the Kuetsjärvi and Kolosjoki sedimentary formations. These cores were drilled during the ICDP FAR-DEEP project. The Kuetsjärvi Sedimentary Formation spans the time interval covering the LJIE and .also includes various carbonate precipitates, which were likely deposited from thermal deep-sourced waters. The Kolosjoki Sedimentary Formation records the return to normal conditions in the aftermath of the LJIE.

The FAR-DEEP drillcore 5A from the Kuetsjärvi Sedimentary Formation yielded a generally upwards decreasing $\delta^{13}C$ trend from ca. 8 to 5‰ (VPDB). This trend was interpreted as primary, as only the contact-altered samples show co-variation between the $\delta^{13}C$ and $\delta^{18}O$ values and the Mn/Sr ratios. An equivalent trend has previously been reported from another drillcore from the same formation. A combined secular $\delta^{13}C$ curve for the Kuetsjärvi Sedimentary Formation was accordingly constructed based on the data from these two cores.

Combined $\delta^{13}C$ data from two FAR-DEEP cores (8A and 8B) from the Kolosjoki Sedimentary Formation show a generally upwards increasing $\delta^{13}C$ trend from ca. -2 to 3‰. Drillcore 8B shows $\delta^{13}C$ values of between -2 and -1‰ in the Hematite member. Both cores show similar upwards increasing $\delta^{13}C$ trends from ca. 1 to 3‰ in the Dolostone member. The Hematite and Dolostone members are separated from one another by the Ferropicrite member. The $\delta^{13}C$ values from the Dolostone member are interpreted as primary. The preservation of primary $\delta^{13}C$ values in the Hematite member is more difficult to establish, but there is no reason to suspect significant post-depositional alteration of the primary $\delta^{13}C$ values.

Drillcore 5A from the Kuetsjärvi Sedimentary Formation contains abundant carbonate precipitates. These include post-depositional cavity and vein fills, and syn-depositional surficial dolomite crusts and cements. These carbonate precipitates commonly show lower $\delta^{13}C$ values than their host carbonates, suggesting the presence of an external carbon source. The $\delta^{13}C$ and $\delta^{18}O$ values show positive co-variation in the precipitates. They also show upwards increasing or decreasing trends in dolomite crusts. In addition, $\delta^{13}C$ and $\delta^{18}O$ values commonly show both upwards and downwards increasing trends from the cavity center. The observed co-variation and the $\delta^{13}C$ and $\delta^{18}O$

trends could indicate a thermal origin, mixing between different fluids, different water/rock-ratios, downwards migration of thermal water and/or evaporation.

Given the lack of evidence for high pCO_2 soils, the most likely explanation for the formation of the cavities and carbonate fills as well as the surficial carbonate precipitates, is deep-sourced CO_2. Geochemical and petrographic data (e.g. feather-shaped crystals) are also consistent with a thermal, deep-sourced origin. The carbonate fills, crusts and cements are interpreted as travertine and "cave travertine".

The results of this PhD study show a generally upwards decreasing $\delta^{13}C$ trend in the final part of the LJIE. This trend likely continued towards negative $\delta^{13}C$ values, which was again followed by a positive $\delta^{13}C$ shift. These $\delta^{13}C$ results and published isotopic age data indicate that the LJIE was followed by a minimum in $\delta^{13}C$ values before 2057 Ma. Precipitation of the inferred thermal travertines in the Kuetsjärvi Sedimentary Formation did not affect the $\delta^{13}C$ values of the host dolostones and limestones.

Acknowledgements

This PhD study was supported by the Väisälä Foundation (Finnish Academy of Science and Letters) and the Finnish Doctoral Program in Geology.

The study was supervised by Professor Juha Karhu, who helped me in many ways through the PhD project and contributed to all my articles. I want to give special thanks to him, for all his support and assistance during the project.

The PhD study also formed a part of the ICDP (International Continental Scientific Drilling Program) FAR-DEEP project (Fennoscandian Arctic Russia – Drilling Early Earth Project). All samples analyzed during this research were provided by FAR-DEEP. I sincerely thank all FAR-DEEP scientists and especially my co-authors Victor Melezhik and Alex Brasier; I also give special thanks to Aivo Lepland, who assisted me during the sampling.

All geochemical and mineralogical analyses were made at the Department of Geosciences and Geography, University of Helsinki. I wish to thank all people who helped me, especially Tuija Vaahtojärvi, Hanna Reijola, Juhani Virkanen, Helena Korkka, Pasi Heikkilä and Radoslaw Michallick.

I was also supported by Anu Kaakinen and Laura Arppe, who were the members of my supervision group. I want to thank them. I am also very grateful to Seija Kultti for the support she gave me. A number of other people also gave me valuable support during my PhD project. It was great to share my ideas and worries with these people.

I want to thank the reviewers and editors of my published papers and the thesis for all valuable comments.

Loving thanks to Katja, who stood by me all these years, giving me much support and consolation.

Three other publications are also related to the PhD project, but have not been included in the thesis:

(1) Brasier, A.E., Salminen, P.E., Melezhik, V.A., Fallick, A.E., 2013. Earth´s Earliest Travertines, in: Melezhik, V.A., Kump, L.R., Fallick, A.E., Strauss, H., Hanski, E.J., Prave, A.R., Lepland, A. (Eds.): Reading the Archive of Earth´s Oxygenation. Volume 3: Global Events and the Fennoscandian Arctic Russia – Drilling Early Earth Project. Springer-Verlag, Berling Heidelberg, Chapter 7.9.4, pp. 1435–1456

(2) Melezhik, V.A., Fallick, A.E., Martin, A.P., Condon, D.J., Kump, L.R., Brasier A.T., Salminen P.E., 2013. The Palaeoproterozoic Perturbation of the Global Carbon Cycle: The Lomagundi-Jatuli Isotopic Event, in: Melezhik, V.A., Kump L.R., Fallick, A.E., Strauss, H., Hanski, E.J., Prave, A.R., Lepland, A (Eds.), Reading the Archive of Earth's Oxygenation, Volume 3: Global Events and the Fennoscandian Arctic Russia – Drilling Early Earth Project. Springer-Verlag, Berlin-Heidelberg. Chapter 7.3, pp. 1111–1150.

(3) Salminen, P.E., Melezhik, V.A., Hanski, E.J., Lepland, A., Romashkin, A.E., Rychanchik, D.V., Luo, Zh.-Y., Sharkov, E.V., Bogina, M.M., 2013. Kuetsjärvi Sedimentary Formation: FAR-DEEP Hole 5A, Neighbouring Quarry and Related Outcrops, in: Melezhik, V.A., Prave, A.R., Fallick, A.E., Hanski, E.J., Lepland, A., R. Kump, L.R. Strauss, H. (Eds.), Reading the Archive of Earth's Oxygenation, Volume 2: The Core Archive of the Fennoscandian Arctic Russia – Drilling Early Earth Project. Springer-Verlag, Berlin-Heidelberg. Chapter 6.2.2, pp. 617–649.

Contents

List of original publications

This thesis is based on the following publications:

I Salminen, P.E., Karhu, J.A., Melezhik, V.A., 2013. Tracking lateral $\delta^{13}C_{carb}$ variation in the Paleoproterozoic Pechenga Greenstone Belt, the north eastern Fennoscandian Shield. Precambrian Research 228, 177–193.

II Salminen, P.E., Karhu, J.A., Melezhik, V.A., 2013. Kolosjoki Sedimentary Formation: a record in the aftermath of the Paleoproterozoic global positive $\delta^{13}C$ excursion in sedimentary carbonates. Chemical Geology 362, 165–180.

III Salminen, P.E., Brasier, A.T., Karhu, J.A., Melezhik, V.A. Travertine precipitation in the Paleoproterozoic Kuetsjärvi Sedimentary Formation, Pechenga Greenstone Belt, NE Fennoscandian Shield. Submitted to Precambrian Research.

The publications are referred to in the text by their roman numerals.

Author´s contributions

The study plans for all these papers were jointly made by J. Karhu and P. Salminen. The drillcore samples were selected by P. Salminen with help of V. Melezhik and A. Lepland. All sample preparation, micro-drilling, analytical work, data processing and statistical analyses were made by P. Salminen. P. Salminen also provided all figures for the articles, excepting the maps, which were modified from the map published by Melezhik and Fallick (2005). P. Salminen prepared the preliminary manuscripts, which were then edited, contributed and commented by co-authors. V. Melezhik also edited the photographs for Paper III.

Abbreviations

DIC	dissolved inorganic carbon
FAR-DEEP	the Fennoscandian Arctic Russia – Drilling Early Earth Project
GOE	the Great Oxidation Event
ICDP	International Continental Scientific Drilling Program
ICP-MS	inductively coupled plasma mass spectrometry
KSF	the Kuetsjärvi Sedimentary Formation (Papers I and III) or the Kolosjoki Sedimentary Formation (Paper II)
KuSF	the Kuetsjärvi Sedimentary Formation
KoSF	the Kolosjoki Sedimentary Formation
LJIE	Lomagundi-Jatuli Isotope Event
PAL	present-day atmospheric level
TDC	total dissolved carbon
VPDB	Vienna Pee Dee Belemnite
XRD	X-ray diffraction
XRF	X-ray fluorescence

List of tables and figures

1 Introduction

The Archean-Paleoproterozoic transition was a time of great global environmental change (Fig. 1; e.g. Melezhik et al., 2005a; Melezhik and Lepland, 2006). One of the most significant events at this time was the rise in atmospheric oxygen (e.g. Bekker et al., 2004; Holland, 2002), known as the Great Oxidation Event (GOE; e.g. Holland, 2002). Another major event was a global perturbation in the carbon cycle, evidenced by a positive $\delta^{13}C$ excursion in sedimentary carbonates (e.g. Karhu and Holland, 1996), referred to as the Lomagundi-Jatuli Isotope Event (LJIE). Other events at the Archean-Paleoproterozoic transition include the deposition of C_{org}-rich sediments (e.g. Condie et al., 2001; Melezhik et al., 1999a, 2004b) and several global "icehouse" events (e.g. Evans, 2003; Evans et al., 1997; Young et al., 2001). This time interval was also characterized by world-wide deposition of banded iron formations (BIFs; e.g. Cloud, 1968; Ohmoto et al., 2006; Pickard, 2003), the first phosphorites (e.g. Bekker et al., 2003a; Maheshwari et al., 2010; Papineau, 2010), abundant marine Ca-sulfates (e.g. Bekker et al., 2006; Schröder et al., 2008) and significant seawater sulfate reservoirs (e.g. Canfield, 2005; Melezhik et al., 2005c; Reuschel et al., 2012). Several petrological and tectonic events also occurred during the Archean-Paleoproterozoic transition, including "the crystal age gap" (Condie et al., 2009) and the break-up of the Neoarchean supercontinent (e.g. Aspler and Chiarenzelli, 1998; Condie et al., 2001, 2009). The Earth´s surface environment at the Archean-Paleoproterozoic transition differed remarkably from that of the modern Earth.

In order to investigate the Archean-Paleoproterozoic transition, the ICDP (International Scientific Drilling Program) FAR-DEEP project (Fennoscandian Arctic Russia – Drilling Early Earth Project) drilled several drillholes in sedimentary successions in the Russian part of the Fennoscandian Shield (Kola, Imandra and Onega regions). These cores have been used in establishing a well characterized and dated sedimentological, isotopic and geochemical archive for the time period 2500–2000 Ma. Excluding banded iron formations, all other global events of the Archean-Paleoproterozoic transition are recorded in Russian Fennoscandia (Melezhik and Lepland, 2006).

This PhD study focused on the FAR-DEEP cores from the Kuetsjärvi and Kolosjoki sedimentary formations of the Pechenga Greenstone Belt (the Kola Peninsula), NW Russia. The Kuetsjärvi Sedimentary Formation (KuSF) was deposited during the time interval bracketing the LJIE, whereas the younger Kolosjoki Sedimentary Formation (KoSF) was deposited during the aftermath of this event. Sedimentary dolostones and limestones were analyzed for C and O stable isotope composition, whole-rock element abundances and selected acid-soluble elements. Detailed $\delta^{13}C$ curves for both formations were constructed to provide more information about the termination of the LJIE.

In addition to background stratified dolostones and limestones, carbonate precipitates in the drillcore from the KuSF were also investigated. These precipitates include cavity and vein fills and surficial dolomite crusts and cements. These precipitates were investigated in detail to provide information about their origin and the depositional setting of the KuSF. The results of this investigation also shed more light on the identification and characterization of different kind of Precambrian carbonate precipitates (e.g. travertine, tufa and speleothems).

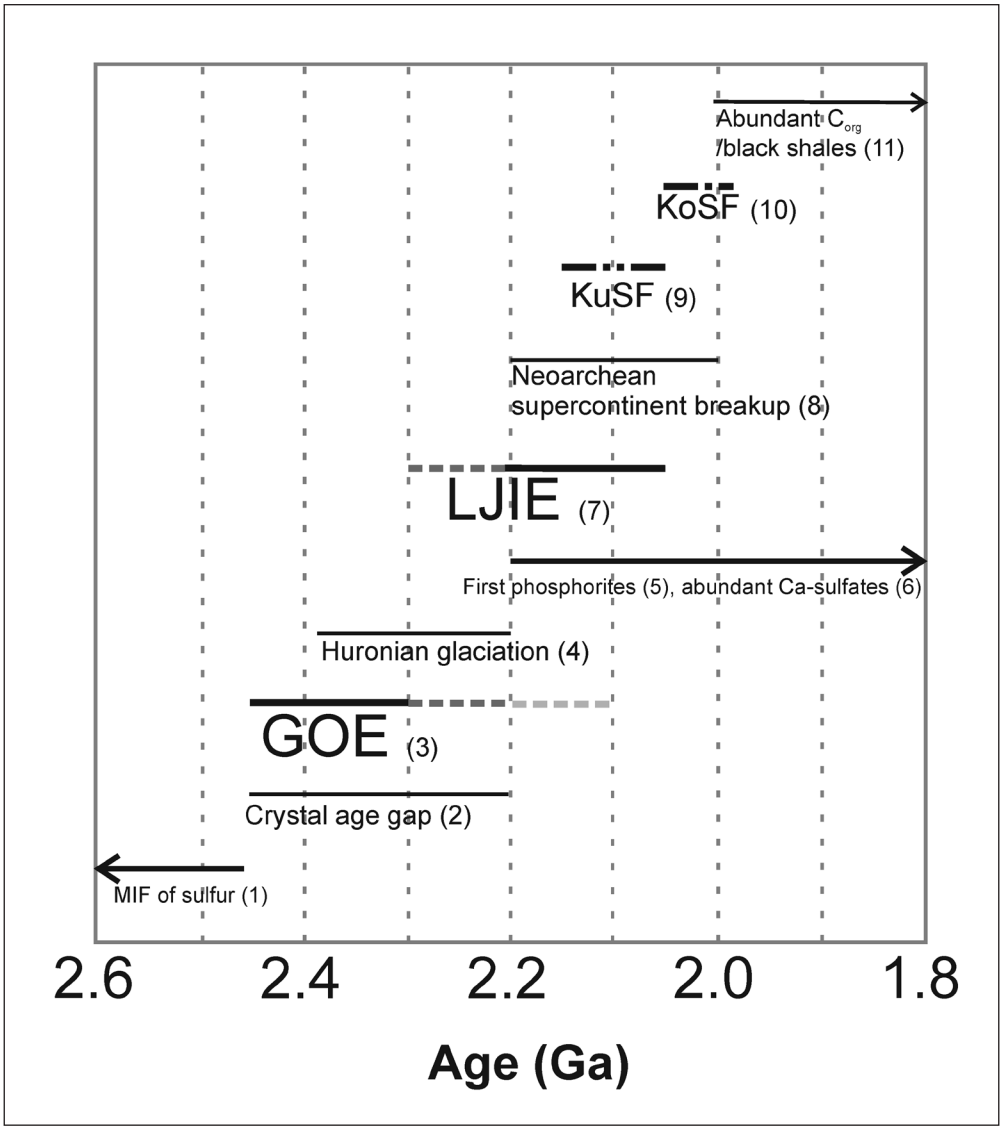

Figure 1. The approximate timing of some key events during the Archean-Paleoproterozoic transition (MIF = Mass-independent sulfur isotope fractionation; LJIE = the Lomagundi-Jatuli Isotope Event; GOE = the Great Oxidation Event). The approximate depositional times of the Kuetsjärvi (KuSF) and Kolosjoki (KoSF) sedimentary formations are also shown. References: (1) Bekker et al., 2004; Farquhar et al., 2000; Guo et al., 2009; (2) Condie et al., 2009; (3) e.g. Bekker et al., 2004, Guo et al., 2009; (4) e.g. Evans et al., 1997; (5) e.g. Bekker et al., 2003a; Maheshwari et al., 2010; Papineau, 2010; (6) e.g. Bekker et al., 2006; Schröder et al., 2008; (7) e.g. Karhu and Holland, 1996, Melezhik et al., 2013a; (8) e.g. Aspler and Chiarenzelli, 1998; Condie et al., 2001, 2009; (9) Amelin et al., 1995; Melezhik et al., 2007; (10) Hanski et al., 1990; Martin et al., 2013b; Melezhik et al., 2007; (11) e.g. Condie et al., 2001; Gauthier-Lafaye and Weber, 2004; Melezhik et al., 1999a, 2004b.

1.1 Isotopic composition of carbon in sedimentary carbonates

The analysis of the isotope composition of carbon in sedimentary dolostones, limestones as well as carbonate precipitates was the main objective of this PhD study. The characteristics of, and controls on the variation of the carbon isotope ratios are described below.

Carbon has two stable isotopes: ^{12}C and ^{13}C. The C isotope composition is usually reported using conventional δ-notation ($\delta^{13}C$), defined as:

$$(1) \qquad \delta = (R_x - R_{std})/R_{std} * 1000$$

where R is the ratio of the abundance of the heavy to that of light isotope. R_x is the isotope ratio in the sample and R_{std} is the ratio in the standard. For carbon, R stands for the ratio $^{13}C/^{12}C$ and the standard is VPDB (Vienna Pee Dee Belemnite). The unit of the δ-value is ‰.

Lithological screening of samples is important when trying to obtain the least altered C isotope composition. The preservation of primary C isotope signals in sedimentary carbonate rocks can also be tested by investigating the co-variation of the $\delta^{13}C$ values with respective $\delta^{18}O$ values and Mn/Sr ratios. The $\delta^{18}O$ value is calculated from the ratio of abundance of ^{18}O to ^{16}O ($^{18}O/^{16}O$). When studying sedimentary carbonate rocks, the standard generally used for $\delta^{18}O$ is VPDB.

Metamorphic processes typically cause a decrease in $\delta^{13}C$ values and leads to coupled ^{13}C and ^{18}O depletions (Valley, 1986). However, carbonates may retain the isotopic signature of the pre-metamorphic material, providing that the de-carbonization reactions are not significant (e.g. Schidlowski et al., 1983, p. 157). Diagenesis normally lowers the $\delta^{18}O$ values, but diagenetic fluids usually contain only traces of carbon and thus do not have significant influence on the $\delta^{13}C$ values (e.g. Emrich et al., 1970). The formation of ^{13}C-depleted methane in anoxic, sulfate depleted sediments can increase the $\delta^{13}C$ values in the sedimentary carbonates (e.g. Hudson, 1977; Irwin et al., 1977).

Ratios of Mn/Sr can be used to estimate the effect of meteoric diagenesis on the primary carbon isotope composition (e.g. Kaufman and Knoll, 1995; Veizer, 1983). When sedimentary carbonate rocks are affected by meteoric waters, they are usually depleted in Sr and enriched in Mn, resuilting in high Mn/Sr ratios. Kaufman and Knoll (1995) proposed that Mn/Sr ratios of >10 imply post-depositional alteration in Neoproterozoic rocks, whereas Melezhik et al. (1999b, 2005b) suggested that Mn/Sr ratios of >6 imply post-depositional alteration in Paleoproterozoic dolostones. Some caution needs to be taken exercised when considering Mn/Sr rations in Paleoproterozoic rocks, as they may have formed in anoxic oceans enriched in Fe^{2+} and Mn^{2+} (e.g. Bekker et al., 2001; Veizer et al., 1992). Moreover, dolostones generally include more Mn and less Sr than limestones (e.g. Gaucher et al., 2007).

Earth´s carbon cycle is very complex. The largest carbon reservoir is the mantle, with a $\delta^{13}C$ value of about -5‰ (e.g. Anderson and Arthur, 1983; Deines, 2002). The two main terrestrial carbon reservoirs are sedimentary carbonate rocks and organic carbon. The relationship between them can be expressed by an isotope mass balance equation (e.g. Broecker, 1970; Des Marais, 2001; Des Marais et al., 1992b; Shidlowski et al., 1983, Summons and Hayes, 1992):

$$(2) \qquad \delta_{carb} = \delta_{in} + f_{org}\Delta_c$$

where Δ_c is the isotopic (δ) difference between the coevally sequestered organic and inorganic (carbonates) carbon during sedimentation, f_{org} is the fraction of organic carbon sequestered, δ_{carb} refers to carbonate sediments and δ_{in} to carbon influx (carbon from volcanism, metamorphism, weathering). The δ_{in} is often taken as -5‰, which is the average value for crustal carbon (Holser et al., 1988) as well as being representative of the mantle value (e.g. Anderson and Arthur, 1983; Deines, 2002). Based on that assumption, the isotope mass balance equation can be expressed in the following format:

(3) $x(\delta^{13}C)_{carbonate}+(1-x)(\delta^{13}C)_{organic\ carbon} = -5‰$

where x is the fraction of carbonate relative to total carbon during carbon burial. The fractionation between inorganic and organic carbon is very large. Sedimentary carbonates normally have $\delta^{13}C$ values ranging from 0 to 1‰ (e.g. Anderson and Arthur, 1983). Organic carbon shows lower $\delta^{13}C$ values, with a mean value at -23‰ (e.g. Anderson and Arthur, 1983).

Photosynthetic fixation of carbon to organic matter shows a preference for the lighter ^{12}C (e.g. Anderson and Arthur, 1983; O´Leary, 1981). When high amounts of organic carbon are buried, the $\delta^{13}C$ values of DIC (dissolved inorganic carbon) and sedimentary carbonates tend to increase. Marine carbonates usually precipitate in near equilibrium with DIC and the fractionation during precipitation is small and relatively insensitive to temperature (e.g. Anderson and Arthur, 1983; Emrich et al., 1970). The average oceanic $\delta^{13}C$ value for total dissolved carbon (TDC) is ca. 0‰, but the surface water TDC commonly shows $\delta^{13}C$ values from 1 to 3‰ (Anderson and Arthur, 1983). The $\delta^{13}C$ values of carbonates are enriched by only 1-2‰ in relation to the oceanic TDC (Anderson and Arthur, 1983).

1.2 The Lomagundi-Jatuli Isotope Event (LJIE) and its aftermath

Chemostratigraphy can be used as a correlation tool in the Proterozoic, where biostratigraphic correlation methods are gemerally inapplicable (e.g. Sial et al., 2010). A secular $\delta^{13}C$ curve can be constructed by analyses of the $\delta^{13}C$ values of the samples from different depths, each depth representing a specific age. The $\delta^{13}C$ curves can be used in correlating distant sections, as the $\delta^{13}C$ values of the marine sedimentary carbonates mirror the $\delta^{13}C$ values of DIC in seawater at the time of their precipitation (e.g. Anderson and Arthur, 1983; Des Marais, 2001; Holser et al., 1988; Scholle and Arthur, 1980).

The residence time of DIC in the oceans is longer than the mixing time of the oceans and the carbon isotope composition of the oceans is relatively homogeneous at any given time. Over longer timescale (e.g. 30 – 100 million years), the global $\delta^{13}C$ value of DIC is controlled by the relative proportions of organic carbon and carbonate in buried carbon (e.g. Keith and Weber, 1964; Scholle and Arthur, 1980). Variations are related to tectonic activity and changes in the degree of primary production.

The exact shape of the Paleoproterozoic secular $\delta^{13}C$ curve is not known. A single positive carbon isotope excursion at ca. 2200–2100 Ma has been recognized (Karhu and Holland, 1996), but its detailed nature is still inadequately constrained. For chemostratigraphic purposes, it is therefore important to obtain more information about the Paleoproterozoic $\delta^{13}C$ evolution. The secular $\delta^{13}C$ curve is also linked to the oxygenation of the atmosphere (see the subsection 1.3).

Sedimentary carbonates extremely enriched in ^{13}C were deposited worldwide at ca. 2200–2100 Ma (e.g. Karhu and Holland, 1996). These carbonates record the Paleoproterozoic global positive $\delta^{13}C$ excursion in sedimentary carbonates, which provides evidence for a major perturbation in the global carbon cycle (e.g. Baker and Fallick, 1989a, 1989b). This positive isotope excursion has become known was the Lomagundi-Jatuli Isotope Event. Martin et al. (2013a) constrained a maximum duration of 249 ± 9 Myr (2306 ± Ma to 2057 ± 1 Ma) for the LJIE and a minimum duration of 128 ± 9.4 Myr (2221 ± 5 Ma to 2106 ± 8 Ma). Martin et al. (2013a) also concluded that a single excursion during the LJIE is permissible, but repeated returns to normal $\delta^{13}C$ values cannot be ruled out (see also Melezhik et al., 1999b).

Carbonates extremely enriched in ^{13}C were

first reported from Jatulian units in Russian Karelia (Galimov et al., 1968), in the Peräpohja Belt of Finland (Schidlowski et al., 1975) and extensively in the Lomagundi Basin, Zimbabwe (Schidlowski et al., 1975, 1976). The LJIE has also been documented in many other localities worldwide (see e.g. Karhu, 1993; Martin et al., 2013a). These include Scotland (Baker and Fallick, 1989a), Ukraine (Zagnitko and Lugovaya, 1989), North-America (e.g. Bekker et al., 2003a; Melezhik et al., 1997), South-America (e.g. Bekker et al., 2003b), Africa (e.g. Bekker et al., 2001; Buick et al., 1998), Australia (Lindsay and Brasier, 2002), India (e.g. Maheswari et al., 1999; Sreenivas et al., 2001) and China (Tang et al., 2011). Several additional sedimentary carbonate successions in the Fennoscandian Shield also document the LJIE, in Norway (Baker and Fallick, 1989b; Melezhik and Fallick, 1996), Finland (e.g. Karhu, 1993), Sweden (Karhu, 1993; Melezhik and Fallick, 2010) and both Karelia and the Kola Peninsula in NW Russia (e.g. Karhu, 1993; Karhu and Melezhik, 1992; Melezhik et al., 1999b; Melezhik and Fallick, 1996; Yudovich et al., 1991).

The KuSF of the Pechenga Greenstone Belt was deposited during the time interval bracketing the LJIE. Several investigations have reported high $\delta^{13}C$ values in the sedimentary carbonates of the KuSF, ranging from 2 to 10‰ (e.g. Karhu, 1993; Karhu and Melezhik, 1992; Melezhik et al., 2003, 2004a; Melezhik and Fallick, 1996, 2001, 2003). Melezhik et al. (2005b) reported a decreasing trend upwards through the stratigraphy from 8.9 to 5.8‰ with several short-term positive and negative spikes (up to 1.7‰).

On a global scale, high $\delta^{13}C$ values can usually be explained by an increased burial fraction of organic carbon (Broecker, 1970; Jenkyns, 1988; Summons and Hayes, 1992). At a more local scale, several other factors can explain ^{13}C enrichment. These include (i) high bio-production in a closed basin (e.g. Bein, 1986; Botz et al., 1988; Hollander and McKenzie, 1991), (ii) stromatolite build-up (e.g. Burne and Moore, 1987; Des Marais et al., 1992a), (iii) intense evaporation in a hypersaline environment (e.g. Friedman, 1998; Stiller et al., 1985), (iv) fermentative diagenesis (e.g. Irwin et al., 1977) and (v) the activity of hot springs (e.g. Friedman, 1970). Excessive bio-production in a closed basin could also result in basin-wide ^{13}C enrichment.

Most of the carbonates recording the LJIE have been found in shallow-water or relatively well-oxygenated settings, which are relatively poor in organic carbon (e.g. Bekker et al., 2008). A couple of investigations (Bekker et al. 2008; Maheswari et al., 2010) have reported C_{org}-rich deep-marine sediments that are coeval with the LJIE. In addition, abundant C_{org}-rich sediments appear to have been deposited after the LJIE in many localities (e.g. Condie et al., 2001; Gauthier-Lafaye and Weber, 2003; Melezhik et al. 1999a, 2004b).

Based on a limited number of data points, Karhu and Holland (1996) recognized a shallow $\delta^{13}C$ minimum after the LJIE at ca. 2000 Ma, followed by a subtle increase in $\delta^{13}C$ at 2000–1900 Ma. Kump et al. (2011) reported a larger negative $\delta^{13}C$ shift in the carbonate rocks and organic matter in the 2090–1980 Ma Zaonega Formation of the Onega Basin, SE Fennoscandia. That $\delta^{13}C$ shift was correlated with a similar $\delta^{13}C$ shift in the 2080–2050 Ma C_{org}-rich shales of the Francevillian Series in Gabon (Gauthier-Lafaye and Weber, 2003). Kump et al. (2011) suggested that this negative $\delta^{13}C$ shift may be global and could be explained by intense oxidation of organic carbon deposited during the Great Oxidation Event.

The 2057 Ma KoSF is important, as it was deposited immediately after the LJIE, and the carbon isotope records from it can be used to test the global significance of the data published by

Kump et al. (2011). Prior to this study, $\delta^{13}C$ values ranging from -8 to 2‰ have been reported from the KoSF (Karhu, 1993; Karhu and Melezhik, 1992; Melezhik et al., 2007; Melezhik and Fallick, 1996; Pokrovskii and Melezhik, 1995).

1.3 The Great Oxidation Event (GOE)

The evolution of $\delta^{13}C$ is directly linked to the oxygenation of the atmosphere. The reduction of inorganic carbon (CO_2) to organic carbon (CH_2O) releases oxygen. When large amounts of organic carbon are buried, the oxygen levels of the atmosphere and oceans tend to rise (e.g. Karhu and Holland, 1996). The increased burial fraction of organic carbon leads to concominant increase in the $\delta^{13}C$ values of sedimentary carbonates (e.g. Karhu and Holland, 1996).

At ca. 2450–2320 Ma, the oxygen level in the Earth´s atmosphere rose significantly (Bekker et al., 2004; Guo et al., 2009), in an event known as the Great Oxidation Event (e.g. Holland, 2002). During the Great Oxidation Event (GOE), the pO_2 likely increased from $<10^{-5}$ to $>10^{-2}$ PAL (PAL = present-day atmospheric level) (Pavlov and Kasting, 2002).

The GOE has been recorded as changes in the oxidation state of paleosols (Holland, 1992), the appearance of red beds (e.g. Bekker et al., 2005; Chandler, 1980; Cloud, 1968), and the disappearance of detrital pyrite, siderite and uraninite in conglomerates (e.g. Rasmussen and Buick, 1999). The appearance of first eukaryotes also indicates higher oxygen levels (e.g. Brocks et al., 1999; Han and Runnegar, 1992). The appearance of first extensive sulfate evaporite beds can also be linked to the formation of oxygenated atmosphere (e.g. Bekker and Holland, 2012). The increase in Mo enrichment in black shales apparently occurred ca. 200 Ma after the GOE (e.g. Scott et al., 2008). Moreover, mass-independent sulfur isotope fractionation was more probably recorded in sediments in a low-pCO_2 atmosphere (Bekker et al., 2004; Farquhar et al., 2000; Guo et al., 2009). The formation of the extensive banded iron formations (BIFs) ceased at the time of the GOE, but it is unclear whether this is a truly diagnostic indicator of oxidation of the atmosphere and oceans (e.g. Canfield, 1998; Ohmoto et al., 2006)

The growth of atmospheric oxygen has been divided into three stages (e.g. Holland, 2006; Kasting, 1987). During Stage 1 (a reducing state), free oxygen would not have been present in either atmosphere or oceans. During Stage 2 (a rapidly oxidizing state), large amounts of oxygen enter the atmosphere and surface ocean waters; the GOE defines Stage 2. During Stage 3 (an aerobic state), free oxygen also enters the deep ocean waters. Stage 3 also includes the "Second Great Oxidation Event" (Campbell and Squire, 2010), which was caused by increased burial of organic carbon between the Neoproterozoic glaciations coinciding with the Snowball Earth. A "one-stage" model has also been presented, suggesting relative constant oxygen levels in the atmosphere for 4 Ga (e.g. Ohmoto et al., 2006), but more evidence seems to support the three-stage model.

Free oxygen (O_2) is accumulated in the atmosphere due to several processes: (i) photosynthesis and burial of organic carbon, (ii) burial of pyrite, (iii) reduction of carbonates and sulfates during diagenesis, (iv) photolysis of H_2O, and (v) escape of hydrogen from the atmosphere (e.g. Catling et al., 2001; Claire et al. 2006; Holland, 2002; Kasting et al., 1993; Kump et al., 2001). In the modern atmosphere, the most important processes are the photosynthesis and burial of organic carbon, whereas the other processes only liberate small amounts of oxygen (e.g. Claire et al., 2006). However, other processes may have been more important in delivering oxygen to the atmosphere prior to the advent of photosynthesis (e.g. Catling et al., 2001; Kasting, 1988).

In modern environments, oxygen is mainly removed from the atmosphere by weathering, respiration and decay of organic matter, and oxidation of volcanic fluids (e.g. Claire et al., 2006; Holland et al., 1986). Oxidation of organic matter consumes most of the O_2 produced by photosynthesis (e.g. Claire et al., 2006; Holland et al., 1986). Thus, burial of organic carbon is necessary to maintain the oxygen in the atmosphere (e.g. Claire et al., 2006). During the Archean, the oxygen sinks may have been larger due to a greater abundance of more reduced volcanic fluids that equilibrated with a lower fO_2 mantle (e.g. Kasting et al., 1993; Kump et al., 2001; Holland, 2002), more reduced metamorphic fluids from a more reduced crust (Catling et al., 2001, Claire et al. 2006) and a lower mean fO_2 of volcanic fluids due to predominance of submarine volcanism (Kump and Barley, 2007).

Several reasons for the GOE have been suggested. The increased oxygen levels were possibly linked to increasing rates of photosynthesis (e.g. Cloud, 1968). The GOE may be connected to the beginning of the cyanobacterial oxygenic photosynthesis (e.g. Kopp et al., 2005). Another alternative is that the oxygen sources exceeded the oxygen sinks (e.g. Kump and Barley, 2007; Kump et al., 2013). One model involves the loss of great amounts of H_2 from the upper atmosphere allowing O_2 to accumulate in the atmosphere (Holland, 2009).

The timing of the Lomagundi-Jatuli Isotope Event in relation to the Great Oxygenation Event is problematic. The LJIE has been constrained to ca. 2200–2060 Ma. Thus, it is apparently post-dating the GOE. According to the compilation of Melezhik et al. (2013a), the LJIE could have started already at ca. 2300 Ma. Martin et al. (2013a) also suggest that the LJIE may have started already at 2306 ± 9 Ma. Still, the LJIE seems to slightly post-date the beginning of the GOE. Bekker and Holland (2012) suggested that the time interval from ca. 2400 to 2220 Ma probably included short-duration positive and negative carbon isotope excursions.

1.4 Travertines, tufas and speleothems

In addition to stratified dolostones and limestones, one of the studied drillcores (Drillcore 5A) includes chemical precipitates – probably representing travertines. Precambrian travertines, tufas and speleothems are rare or have not been confidently identified (e.g. Brasier, 2011). Identifying them and distinguishing between different types of Precambrian carbonate precipitates is challenging. For example, discriminating between tufas (ambient water precipitates) and travertines (thermal water precipitates) is difficult, because there were no macrophytes in Precambrian time. Precambrian sedimentary rocks have also been exposed to different post-depositional alteration processes, including diagenesis and metamorphism. Moreover, the words "tufa" and "travertine" have diverse and multiple meanings. Thus, it is important to carefully describe the different kinds of carbonate precipitates.

Classically, the word "tufa" was used for both volcanic ash and soft, poorly consolidated freshwater carbonates, but later the word "calcareous tufa" was applied to freshwater carbonates (e.g. Pentecost and Viles, 1994). The word "calcareous tufa" and "tufa" are now used for the softer varieties, whereas the word travertine is used for the harder freshwater carbonates (e.g. Pentecost and Viles, 1994). Travertines and tufas have also been classified based on their fabrics, morphology, geochemistry and depositional temperature (e.g. Ford and Pedley, 1996; Pentecost and Viles, 1994).

Some authors have used the word "travertine" to describe both chemical precipitates from

thermal water (thermogene travertine) and ambient water chemical precipitates (meteogene travertine) (e.g. Pentecost and Viles, 1994). However, European authors commonly use the word "travertine" only for thermal water precipitates, whereas the word "tufa" is used for the ambient water precipitates (see e.g. Ford and Pedley, 1996). In this study, the word "travertine" is used for thermal water precipitates.

Speleothems are found in subterranean situations, lining caves and fracture systems (e.g. Pedley and Rogerson, 2010). Speleothems include e.g. stalactites, stalagmites, helictites and flowstones (e.g. Ford and Williams, 2007, p. 281). Speleothems are regarded as precipitates formed purely by physico-chemical processes, although they may be found in settings where also biologically-induced carbonate precipitation occurs (e.g. Pedley and Rogerson, 2010). Modern speleothems are usually formed under high pCO_2 subsurface conditions (e.g. Fairchild et al., 2000). However, Precambrian speleothems were formed in some other way, as there were no high pCO_2 soils at that time. Some Precambrian karst and speleothems may have been formed due to the common-ion effect caused by dissolution of evaporites (e.g. Calaforra et al., 2008; Wigley, 1973a) or incongruent dissolution of dolomites (e.g. Wigley, 1973b). Deep-sourced CO_2 could also explain the formation of karst and speleothems without requiring high pCO_2 soils (e.g. Duliński et al., 1995; Pentecost and Viles, 1994; Yoshimura et al., 2004). Other processes may also have formed the Precambrian karst and speleothems (see e.g. Brasier, 2011).

The cave/cavity deposits may also have a thermal origin (e.g. Corbella et al., 2004; Djidi et al., 2008; Dublyansky, 1995). The words "travertine" or "tufa" have sometimes been restricted to sub-aerial settings, but they have been applied to subsurface settings as well. Thus, the name "cave travertine" could be used for cave/cavity deposits, that precipitated from deep-sourced thermal water.

Modern (thermogene) travertines are characterized by $\delta^{13}C$ values varying from -4 to 8‰ (e.g. Chafetz and Lawrence, 1994; Friedman, 1970; Pentecost and Viles, 1994; Renaut and Jones, 1997). In contrast, tufas (meteogene travertine) usually show $\delta^{13}C$ values varying from -11 to 0‰ (e.g. Usdowski et al., 1979; Chafetz and Lawrence, 1994; Pentecost and Viles, 1994). Ambient water speleothems show relatively similar $\delta^{13}C$ values to those in tufas (e.g. Pentecost, 2005, p. 142).

1.5 Publications: aims of the study

Paper I: Specification of the carbon isotope curve of the Kuetsjärvi Sedimentary Formation (Drillcore 5A)

One of the main goals of this PhD study was the construction of a detailed secular $\delta^{13}C$ curve for the Kuetsjärvi Sedimentary Formation, which was deposited during the LJIE. New data was provided by analyzing several sedimentary carbonate rock samples from different depths in Drillcore 5A. The newly obtained data from Drillcore 5A were compared to those previously obtained from another drillcore (Drillcore X) by Melezhik et al. (2005b). A combined secular $\delta^{13}C$ curve was constructed based on the data from these two drillcores. The meaning of this curve in the global context was discussed.

Paper II: Specification of the carbon isotope curve of the Kolosjoki Sedimentary Formation (Drillcores 8A and 8B)

A detailed secular $\delta^{13}C$ curve for the Kolosjoki Sedimentary Formation was constructed by analyzing sedimentary carbonate samples from different depths in Drillcores 8A and 8B. A combined secular $\delta^{13}C$ curve was constructed based on the $\delta^{13}C$ data from these two cores. Global correlations were made and the meaning

of the combined $\delta^{13}C$ curve was discussed. The KoSF was deposited during the aftermath of the LJIE.

Paper III: Investigation of cavity and vein precipitates and surficial precipitates in the Kuetsjärvi Sedimentary Formation (Drillcore 5A)

In addition to stratified dolostones and limestones, Drillcore 5A includes abundant carbonate precipitates in cavities and veins and on bedding surfaces, subaerial erosional surfaces and surface rock fragments. The nature of these precipitates was examined by analysis of e.g. C isotope geochemistry. Previously, similar kinds of surficial crusts and some cavity fills had been interpreted as travertines deposited by hot-springs (Melezhik et al., 2004; Melezhik and Fallick, 2001). The goals of this new investigation were to (i) determine the origins of these precipitates in the KuSF, (ii) shed more light on the identification of different Precambrian carbonate precipitates, and (iii) provide more information about the depositional setting of the KuSF. The reconstruction of the paleoenvironment of the KuSF is important for obtaining more information about the Earth´s surficial environments during the LJIE.

2 Geological setting

This PhD thesis is based on drillcore samples, which were obtained from three ICDP FAR-DEEP drillcores. These drillcores were drilled from Paleoproterozoic sedimentary formations in the Pechenga Greenstone Belt, NW Russia (Fig. 2). Drillcore 5A was drilled from the Kuetsjärvi Sedimentary Formation, while the partially overlapping Drillcores 8A and 8B were drilled from the Kolosjoki Sedimentary Formation.

The Pechenga Greenstone Belt belongs to a larger (app. 1000 km long) discontinuous volcanic-sedimentary belt in the NE part of the Fennoscandian Shield (e.g. Melezhik and Sturt, 1994). This larger belt has been interpreted as an intracontinental rift, which developed into an intercontinental rift followed by an aborted oceanic phase and an arc-continent collision (e.g. Melezhik and Sturt, 1994). Berthelsen and Marker (1986) suggested more extensive ocean opening followed by oceanic floor subduction and arc-continent collision. The metamorphic grade of the Pechenga Greenstone Belt ranges from prehnite-pumpellyite facies to epidote-amphibolite facies (Petrov and Voloshina, 1995). The rocks in Drillcores 5A, 8A and 8B have been subjected to greenschist facies metamorphism.

The Pechenga Greenstone Belt has been divided into the North and South Pechenga groups (e.g. Melezhik and Sturt, 1994). The Kuetsjärvi and Kolosjoki sedimentary formations belong to the North Pechenga Group, which has been divided (from oldest to youngest) into the Neverskrukk, Ahmalahti, Kuetsjärvi sedimentary, Kuetsjärvi volcanic, Kolosjoki sedimentary, Kolosjoki volcanic, Pilgujärvi sedimentary and Pilgujärvi volcanic formations (Fig. 3) (e.g. Melezhik and Hanski, 2013; Melezhik and Sturt, 1994).

The maximum age constraint for the North Pechenga Group is 2505 ± 1.6 Ma (U-Pb zircon; Amelin et al., 1995), obtained from the Mount Generalskaya gabbronorite intrusion, which is overlain with an erosional discordance by basal conglomerates of the Neverskrukk Formation. The minimum age constraint on the North Pechenga Group is 1970 ± 5 Ma (U-Pb zircon; Hanski et al., 1990) obtained from felsic tuffs of the Pilgujärvi Volcanic Formation. The North Pechenga Group has been interpreted as having accumulated in environments ranging from terrestrial through shallow- to deep-water marine (Berthelsen and Marker, 1986).

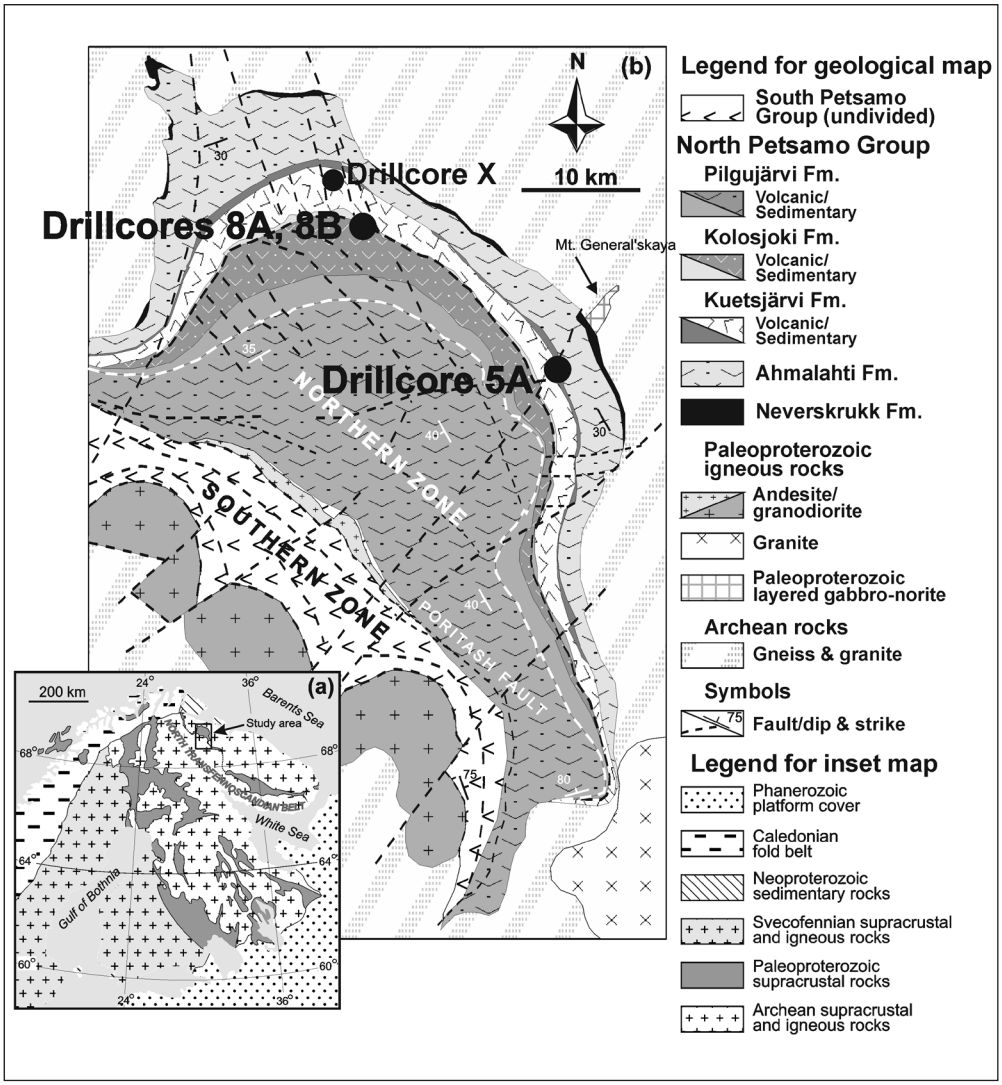

Figure 2. (a) The location of the study area (the Pechenga Greenstone Belt) in the Fennoscandia. (b) The location of the investigated drillcores (5A, 8A and 8B) in the Pechenga Greenstone Belt. Drillcore X, investigated by Melezhik et al. (2005b), is also shown in the map. The maps have been modified from Melezhik and Fallick (2005).

The minimum depositional age of the KuSF and the maximum depositional age of the KoSF is 2058 ± 2 Ma, which is an U-Pb age constrained from detrital zircons in volcaniclastic conglomerates within the overlying Kuetsjärvi Volcanic Formation and volcaniclastic, fluvial and deltaic sediments in the underlying Kolosjoki Sedimentary Formation. The depositional age of the Kolosjoki Sedimentary Formation has recently been further constrained to 2056.6 ± 0.8 Ma from U-Pb analysis of zircons within a fine-grained mafic tuff (Martin et al., 2013b).

The Kuetsjärvi Sedimentary Formation is underlain by the Ahmalahti Volcanic Formation and overlain by the Kuetsjärvi Volcanic Formation (Fig. 3, e.g. Melezhik and Sturt, 1994). The Kuetsjärvi Sedimentary Formation records the Paleoproterozoic global positive

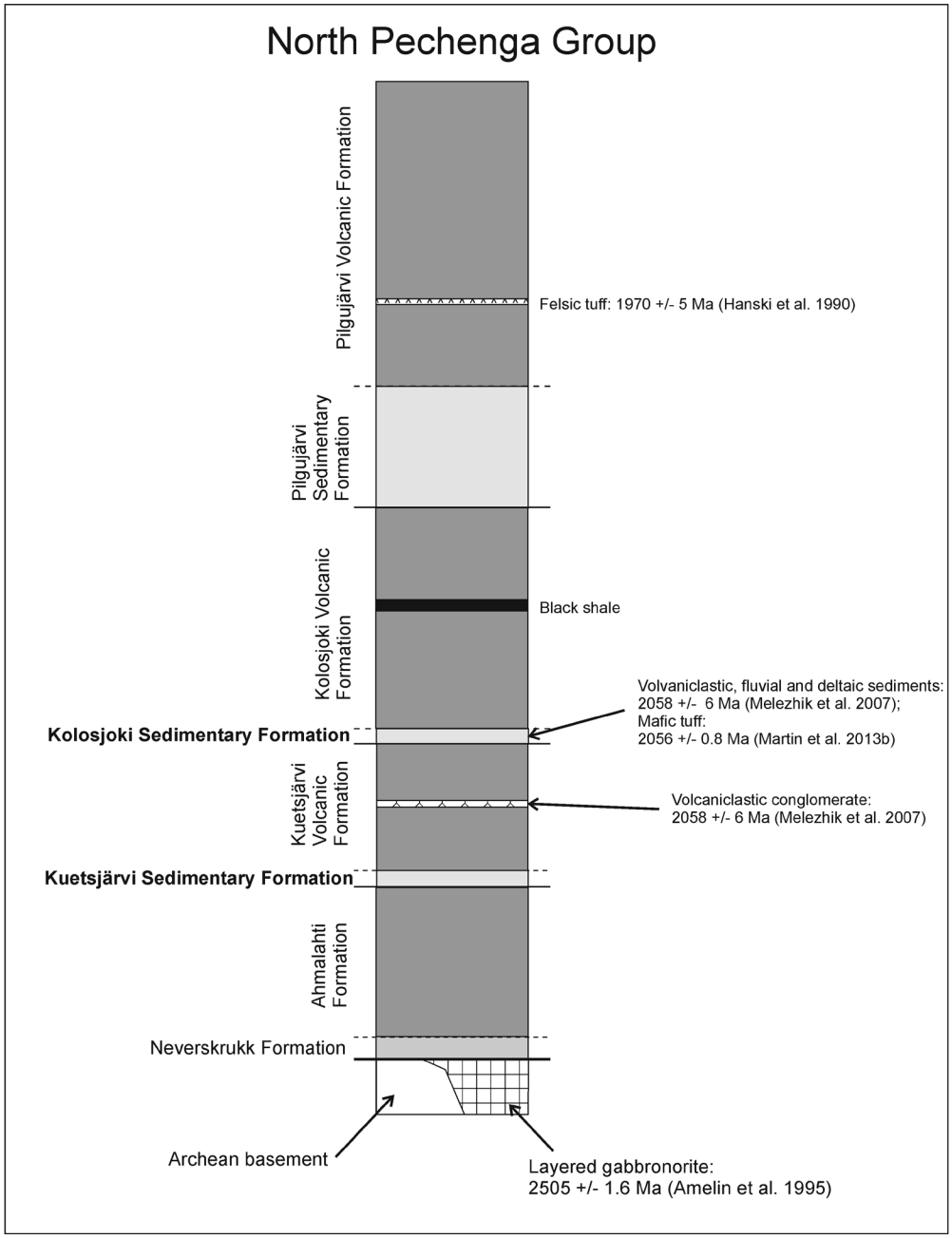

Figure 3. A schematic diagram showing the lithostratigraphy of the North Pechenga Group (modified and simplified from Melezhik et al., 2007).

$\delta^{13}C$ excursion in the sedimentary carbonates, the LJIE. Melezhik and Fallick (2005) divided the KuSF informally into the Quartzite and Dolostone members. The KuSF in Drillcore 5A has been informally divided (from bottom to top) into the Arkosic, Lower Dolostone, Quartzite and Upper Dolostone members (Salminen et al., 2013). There is also ca. 5 m thick Fe-

picrite dyke between the Arkosic and Lower Dolostone members in Drillcore 5A (Salminen et al., 2013). According to Melezhik et al. (2005b) and Melezhik and Fallick (2005), the depositional setting of the KuSF evolved from deltaic through shallow lacustrine to a marine-influenced rift-bounded lake. The KuSF in Drillcore 5A has been interpreted to be have been deposited in a deltaic/delta-front/prodelta and shallow lacustrine environments, which were occasionally tidally influenced (Salminen et al., 2013).

Different carbonate rocks have been identified in the KuSF, including stromatolitic, micritic and sparry dolostones, re-sedimented sandy dolostones, dolarenite, calcarenite, micritic limestone and de-dolomitized dolostone (Melezhik and Fallick, 2005; Salminen et al., 2013). The KuSF also includes precipitates, which have previously been interpreted as travertines associated with hot-spring activity (Melezhik et al., 2004a; Melezhik and Fallick, 2001). Calcrete (caliche), dolocrete, silcrete, silica sinters and small-scale karst have also been recognized (Melezhik et al., 2004a; Melezhik and Fallick, 2001, 2003). Siliciclastic rocks of the KuSF include arkosic siltstone, hematitic mudstone, graywacke and arkosic, quartzitic and tuffitic sandstones (e.g. Melezhik and Fallick, 2005; Salminen et al., 2013). Carbonaceous and dolomitic siliciclastic rocks have also been found (Salminen et al., 2013).

The Kolosjoki Sedimentary Formation is underlain by the Kuetsjärvi Sedimentary Formation and the Kuetsjärvi Volcanic Formation (Fig. 3; e.g. Melezhik et al., 2007). A thrust is separating the KoSF from the overlying Kolosjoki Volcanic Formation (e.g. Melezhik and Hanski, 2013). The Kolosjoki Volcanic Formation is in turn overlain by the Pilgujärvi Sedimentary Formation and Pilgujärvi Volcanic Formation (e.g. Melezhik and Sturt, 1994). The deposition of the KoSF postdates the LJIE. The sediments of the KoSF have been attributed to deposition in fluvial, deltaic and shallow-marine environments (Melezhik et al., 2007, 2013b).

Previously, the KoSF has been informally divided into the Red Bed, Dolostone and Black Shale members (Melezhik et al., 1994). In Drillcores 8A and 8B, the KoSF has been informally divided (from bottom to top) into the Sandstone, Lower Graywacke, Gritstone, Hematite, Ferropicrite, Dolostone and Upper Graywacke members (Melezhik et al., 2013b). Drillcore 8A intersected the entire Dolostone member and it also includes rocks of the Ferropicrite and Upper Graywacke members. Drillcore 8B intersected ca. 310 m of the KoSF as well as ca. 13 m of the underlying Kuetsjärvi Volcanic Formation.

The Sandstone member of the KoSF is characterized by fluvial sandstones (Melezhik et al., 2013b). The Lower Graywacke, Gritstone and Hematite members include siliciclastic deltaic rocks; the Hematite member also includes dolorudite, dolarenite, calcarenite and calcirudite (Melezhik et al., 2013b; Paper II). The Ferropicrite member is comprised of ferropicritic tuff, siltstone and sandstone-siltstone couplets (tuffites) (Melezhik et al., 2013b). The carbonate rocks of the Dolostone member include dolarenite, dolorudite microsparitic and stromatolitic dolostones and stromatolitic limestone (Melezhik et al., 2013b). The Dolostone member also includes graywacke, breccia, arkosic sandstone, gritstone and conglomerate in the upper part of the member (Melezhik et al., 2013b).

3 Materials and methods

All analyses were made at the Department of Geosciences and Geography, University of Helsinki.

Drillcore 5A (KuSF) samples were mainly obtained from the Upper and Lower Dolostone members in the core. In addition, one sample was obtained from the basal part of the Quartzite member; results from this sample were combined with the results from the Lower Dolostone member. All Drillcore 8A (the KoSF) samples were obtained from the Dolostone member. Drillcore 8B (KoSF) samples were obtained from the Hematite and Dolostone members.

Whole-rock samples were used in Papers I and II to provide bulk isotopic and geochemical proxies. Samples were carefully chosen to avoid potential travertines (Drillcore 5A) and other secondary precipitates although they could not be completely avoided. In Paper I (Drillcore 5), micro-drilled samples were used to supplement the whole-rock data and to provide more accurate $\delta^{13}C$ data. In Paper II (Drillcore 8A and 8B), the micro-drilled samples were used to supplement the whole-rock data. Paper III was solely based on data from micro-drilled samples.

The whole-rock samples were analyzed for $\delta^{13}C$ and $\delta^{18}O$, C_{tot}, major oxides (XRF) and selected acid-soluble elements (ICP-MS). All micro-drilled samples from Drillcore 5A were analyzed for $\delta^{13}C$ and $\delta^{18}O$. All micro-drilled host dolostones and limestones and the majority of the micro-drilled "travertines" were also analyzed for acid-soluble elements. The micro-drilled samples from Drillcores 8A and 8B were only analyzed for $\delta^{13}C$ and $\delta^{18}O$ values.

The contents of C_{tot} were determined by a Vario Microcube CNS analyzer. A sulfanilamide standard was used. The precision (1σ) of the analyses was determined by multiple analyses of the reference material (NCS DC73306). The contents of S_{tot} were also analyzed, but S_{tot} levels remained below the detection limit (40 ppm).

The contents of major oxides (SiO_2, Al_2O_3, MgO, CaO, Na_2O, K_2O, P_2O_5) in whole-rock samples were analyzed by a Philips PW1480 X-ray fluorescence spectrometer. The accuracy and the precision (1σ) of the analyses were determined using two reference materials (SARM 40, COQ-1). The accuracy and the precision for Na_2O were not determined, because its content was below the detection limit on most of the drillcore samples and also in one of the reference materials (SARM40).

The acid-soluble elemental (Mg, Ca, Mn, Sr, Fe, Ba) contents were determined using Agilent 7500ce/cx ICP-MS. Sample powder (ca. 9 – 13 mg) was leached in 0.5M acetic acid (5 ml) for 16h at room temperature. The results were calculated in relation to the acid-soluble fraction. The precision (1σ) of the analyses was estimated using duplicate samples and reference materials (SARM 40, COQ-1).

The C and O isotope compositions were determined by a Thermo Finnigan Delta Plus Advantage mass spectrometer in a continuous flow mode. The isotopic composition of the sample powder (125 – 170 μg) was measured from phosphoric-acid-liberated CO_2 gas. The results were expressed using the δ-notation, as per-mil difference from VPDB standard. Reproducibilities (1σ) for $\delta^{13}C$ and $\delta^{18}O$ values were determined using in-house quality standards for dolomite and calcite.

Petrology and mineralogy of the samples (especially carbonate precipitates) were investigated optically in thin sections, visually in hand specimens and qualitatively with an electron micro analyzer.

Depending on the sample type and amount, the carbonate mineralogy (dolomite or calcite) of the samples was determined using (1) XRD analyses, (2) dilute acid-soluble Mg and Ca contents (ICP-MS), and/or (3) acid tests (ca. 1 M HCl).

4 Results and discussion

The isotopic composition of C and O, the elemental composition of the acid-soluble fraction, the XRF data and the contents of C_{tot} of the analyzed samples are shown Tables 1 and 2. In these tables, the average values or variations of the variables are shown for each drillcore (5A, 8A and 8B) and sample type.

4.1 The secular $\delta^{13}C$ curve of the Kuetsjärvi Sedimentary Formation

In Drillcore 5A from the KuSF, the obtained $\delta^{13}C$ values show an upwards decreasing trend from ca. 8 to 5 ‰ (Paper I, Figs. 4, 6). It is considered likely that primary $\delta^{13}C$ values have been preserved, as only the contact altered samples show co-variation between the $\delta^{13}C$ and $\delta^{18}O$ values and the Mn/Sr ratios (Paper I). The samples from the Upper Dolostone member may have been less exposed to post-depositional alteration as they show lower Mn/Sr ratios than the samples from the Lower Dolostone member (Paper I).

The newly obtained $\delta^{13}C$ data from Drillcore 5A were compared to those previously obtained from Drillcore X (Melezhik et al., 2005b). Both cores show a similar upwards decreasing $\delta^{13}C$ trend. The micro-drilled data from Drillcore 5A (Paper I) and the whole-rock data from Drillcore X (Melezhik et al., 2005b) were used to construct a combined secular $\delta^{13}C$ curve for the Kuetsjärvi Sedimentary Formation (Paper I; Fig. 4, 6).

The combined secular $\delta^{13}C$ curve of the KuSF probably represents the final part of the Lomagundi-Jatuli isotopic event (Paper I). Relatively similar $\delta^{13}C$ trends have been reported from other successions world-wide. A $\delta^{13}C$ trend with a similar magnitude was recognized in the middle and upper parts of the succession in the Kalix Greenstone Belt (ca. 2100–1800 Ma) in Sweden (Melezhik and Fallick, 2010). A similar kind of a $\delta^{13}C$ trend was also found in the lower and middle Nash Fork Formation (ca. 2200–1970 Ma), in the Wyoming Craton (Bekker et al., 2003a). Some parts of the FC Formation (> ca. 2080 Ma) of the Francevillian Group also show a comparable $\delta^{13}C$ trend (Préat et al., 2011). The Tulomozero Formation (>1980 Ma) in the northern Onega Lake area, in the Northwestern Russia, shows generally higher $\delta^{13}C$ values than in the KuSF (Melezhik et al., 1999b).

Karhu (1993) also reported ^{13}C enriched carbonates from Finland from three separate successions, including the Kiihtelysvaara section (<2115 Ma), the Kuusamo Schist Belt (<2405 Ma) and the Rantamaa Formation of the Peräpohja Belt (2106 ± 8 Ma; Karhu et al., 2008). All these sections show upwards decreasing $\delta^{13}C$ trends.

The depositional settings of the KuSF in Drillcore 5A were likely marine-influenced lacustrine and deltaic/prodelta/delta-front environments (Salminen et al., 2013). The succession in the Kalix Greenstone Belt as well as that in the Nash Fork Formation have been interpreted to have been deposited in shallow-marine environments (Bekker et al., 2003a; Melezhik and Fallick, 2010). Préat et al. (2011) interpreted the depositional setting of the Francevillian Series as a low-lying sabkha environment with occasional marine flooding. The Tulomozero Formation includes shallow-marine deposits and non-marine "red-beds" (Melezhik et al., 1999b). Its upper part was likely deposited in a tidally influenced environment (Melezhik et al, 1999b). The Kiihtelysvaara section was likely deposited in an epicontinental setting, whereas the carbonates of the Kuusamo Schist Belt and the Rantamaa Formation were likely deposited in a tidal environment (see Karhu, 1993). Thus, it seems that both lacustrine and marine environments show relatively similar

Table 1. XRF data and C_{tot} contents of the samples The data has been adopted or calculated from Papers I-II. The MgO and CaO data for samples from Drillcores 8A and 8B have not been published.

	Average content of the samples or variation in the samples							
	SiO_2 (wt%)	Al_2O_3 (wt%)	MgO (wt%)	CaO (wt%)	Na_2O (wt%)	K_2O (wt%)	P_2O_5 (wt%)	C_{tot} (wt%)
Drillcore 5A, whole-rock samples	15.47	0.88	17.60	26.38	<0.039 - 0.34	<0.008 - 1.46	0.07	10.6
Drillcore 8A, whole-rock samples	15.69	0.80	17.00	26.20	<0.039 - 0.79	<0.008 - 2.60	0.04	10.2
Drillcore 8B, whole-rock samples, Dolostone member	13.60	0.68	17.84	26.65	<0.039 - 0.68	<0.008 - 2.80	0.03	10.8
Drillcore 8B, whole-rock samples, Hematite member	18.04	1.04	9.46	30.19	<0.039	0.64	0.13	9.0

$\delta^{13}C$ evolution. This suggests that the $\delta^{13}C$ curve obtained from the KuSF likely represents a global trend.

As similar $\delta^{13}C$ curves were found in two drillcores separated by a distance of about 25 km, local factors cannot explain the observed $\delta^{13}C$ evolution in the KuSF (Paper I). It is unlikely, that evaporation, for example, could result in similar $\delta^{13}C$ curves in two localities over a distance of 25 km. The ^{13}C enrichment of the KuSF is therefore better explained by basin-wide factors (e.g. extreme bio-production in a closed basin, e.g. Bein, 1986; Botz et al, 1988; Hollander and McKenzie, 1991) or global-scale processes (increased burial of organic carbon; e.g. Jenkyns, 1988).

Most shallow-water carbonates deposited during the LJIE contain only small amounts of C_{org} (e.g. Bekker et al., 2008). The apparent scarcity of C_{org} deposition has been identified as a paradox and presents a problem for the organic carbon burial model (Melezhik et al., 1999b; Melezhik and Fallick, 1996). However, deep-water C_{org}-rich sediments coeval with the LJIE have recently been reported. Bekker et al. (2008) found that the ^{13}C enriched carbonates of the Silverton and Sengoma formations in South Africa and Botswana were associated with deep-water C_{org}-rich shales. They also suggested that the Paleoproterozoic shales in West Africa and Brazil were likewise deposited during the LJIE. Maheswari et al. (2010) reported deep-water C_{org}-rich shales from the Rio Itapicuru Greenstone Belt, Brazil and from Uruguay; these shales were also considered to have been deposited during the LJIE. Thin horizons with less elevated or negative $\delta^{13}C$ values were also found in the Uruguayan sections sections by Maheswari et

Table 2. The isotope composition of C and O and the elemental composition of acid-soluble fraction in the samples. The results have been adopted or calculated from the results in Papers I-III. The Ba contents of the background stratified dolostones and limestones (”host rocks”) in Drillcore 5A have not been published.

	Average value/content of the samples									Variation in the samples
	$\delta^{13}C$ (VPDB, ‰)	$\delta^{18}O$ (VPDB, ‰)	Mg (ppm)	Ca (ppm)	Mn (ppm)	Fe (ppm)	Sr (ppm)	Ba (ppm)	Mn/ Sr	Mg/Ca
Drillcore 5A										
Whole-rock samples (”host rocks”)	7.43	-13.10	129409	200250	455	1912	153	1	4.51	0.43 - 0.68
Micro-drilled subsamples (”host rocks”)	7.50	-13.08	89148	140619	350	1677	129	10	4.65	0.02 - 0.71
Carbonate precipitates (micro-drilled subsamples)	6.75	-12.59	98601	160677	638	1559	96	6	9.40	0.01 - 0.71
Drillcore 8A										
Whole-rock samples	1.96	-11.72	137727	222396	783	4426	63	132	14.01	0.53 - 0.69
Micro-drilled samples	2.31	-11.61								
Drillcore 8B										
Whole-rock samples, Dolostone member	1.95	-10.00	131455	208946	811	3148	32	14	34.26	0.49 - 0.67
Whole-rock samples, Hematite member	-1.43	-15.12	70975	286847	7726	4793	163	6	69.89	0.04 - 0.56
Micro-drilled samples, Dolostone member	1.92	-9.84								
Micro-drilled samples, Hematite member	-1.50	-16.28								

al. (2010), who speculated these horizons could represent negative carbon isotope excursions. Accordingly, the organic carbon burial model can no longer be rejected simply on the basis of a perceived absence of C_{org} deposition during the LJIE.

4.2 The secular $\delta^{13}C$ curve of the Kolosjoki Sedimentary Formation

Drillcore 8A and 8B were investigated to construct a secular $\delta^{13}C$ curve for the Kolosjoki Sedimentary Formation (KoSF) (Paper II). The samples from the Hematite member in Drillcore 8B show $\delta^{13}C$ values between -2 to -1‰ (Paper II). Both cores show an upwards increasing $\delta^{13}C$ trend from ca. 1 to 3 ‰ in the Dolostone member (Paper II). Combined, the two drillcores show an upwards increasing $\delta^{13}C$ trend from ca. -2 to 3‰ (Paper II; Fig. 4). Most of the samples appear to have retained their primary $\delta^{13}C$ composition as only weak correlations were found between the $\delta^{13}C$ and $\delta^{18}O$ values and the Mn/Sr ratios (Paper II).

A combined secular $\delta^{13}C$ curve was constructed based on the $\delta^{13}C$ data from Drillcores 8A and 8B (Paper II; Fig. 4). This curve shows evidence of low $\delta^{13}C$ values after the LJIE, followed by an increase in $\delta^{13}C$ (Paper II). Karhu and Holland (1996) recognized a shallow $\delta^{13}C$ minimum and a subtle increase in $\delta^{13}C$ at ca. 2000–1900 Ma. Paper II reports an even greater $\delta^{13}C$ shift constrained to have occurred at 2058-1970 Ma and provides more support for the global nature of the increasing $\delta^{13}C$ trend.

Melezhik et al. (2007) also reported a similar kind of upwards increasing $\delta^{13}C$ trend in a third drillcore (Drillcore IX) from the KoSF. The results from this core were not included in the secular $\delta^{13}C$ curve, as the results have not been placed within their appropriate lithostratigraphical context. Nevertheless, the results from Drillcore IX support the findings of Paper II.

The $\delta^{13}C$ minimum and increasing $\delta^{13}C$ trend found in Drillcores 8A and 8B could be explained by variations in the burial fractions of organic carbon (see Paper II). According to the isotope mass balance model, highly positive $\delta^{13}C$ values are linked to a high fraction of organic carbon burial and low $\delta^{13}C$ values to a low fraction of organic carbon burial (e.g. Broecker, 1970; Jenkyns, 1988; Summons and Hayes, 1992). The increasing $\delta^{13}C$ trend in the KoSF could therefore be linked to an increasing amount of burial of organic carbon after the LJIE. Abundant C_{org}-rich sediments were deposited coevally (ca. 2100–1950 Ma) to the deposition of the KoSF (e.g. Condie et al., 2001; Gauthier-Lafaye and Weber, 2003; Melezhik et al. 1999a, 2004b). Alternatively, the positive $\delta^{13}C$ shift of the KoSF could also represent recovery from the disturbance caused by an increase in atmospheric oxygen abundances and associated preferential weathering of sedimentary organic matter (Paper II; see also Kump et al., 2011). The role of possible gas hydrates (e.g. Hag, 1998; Kvenvolden, 1999) in mediating the low $\delta^{13}C$ values should be considered as well; dissociation of gas hydrates would release methane with extremely low $\delta^{13}C$ values (e.g. Dickens et al., 1995; Kvenvolden, 1993).

Kump et al. (2011) found evidence of extremely negative $\delta^{13}C$ values (down to -20‰) in the Zaonega Formation (the Lake Onega Basin, SE Fennoscandian Shield), the deposition of which occurred in the same time period of that of the KoSF. They correlated this negative $\delta^{13}C$ shift to that found in the Francevillian Series in Gabon (Gauthier-Lafaye and Weber, 2003) and thus suggested that this shift might be global in character. The isotope mass balance model alone cannot explain $\delta^{13}C_{carb}$ values lower than -5‰, whereas preferential decomposition of sedimentary organic matter under an oxidizing atmosphere deposited during the LJIE might

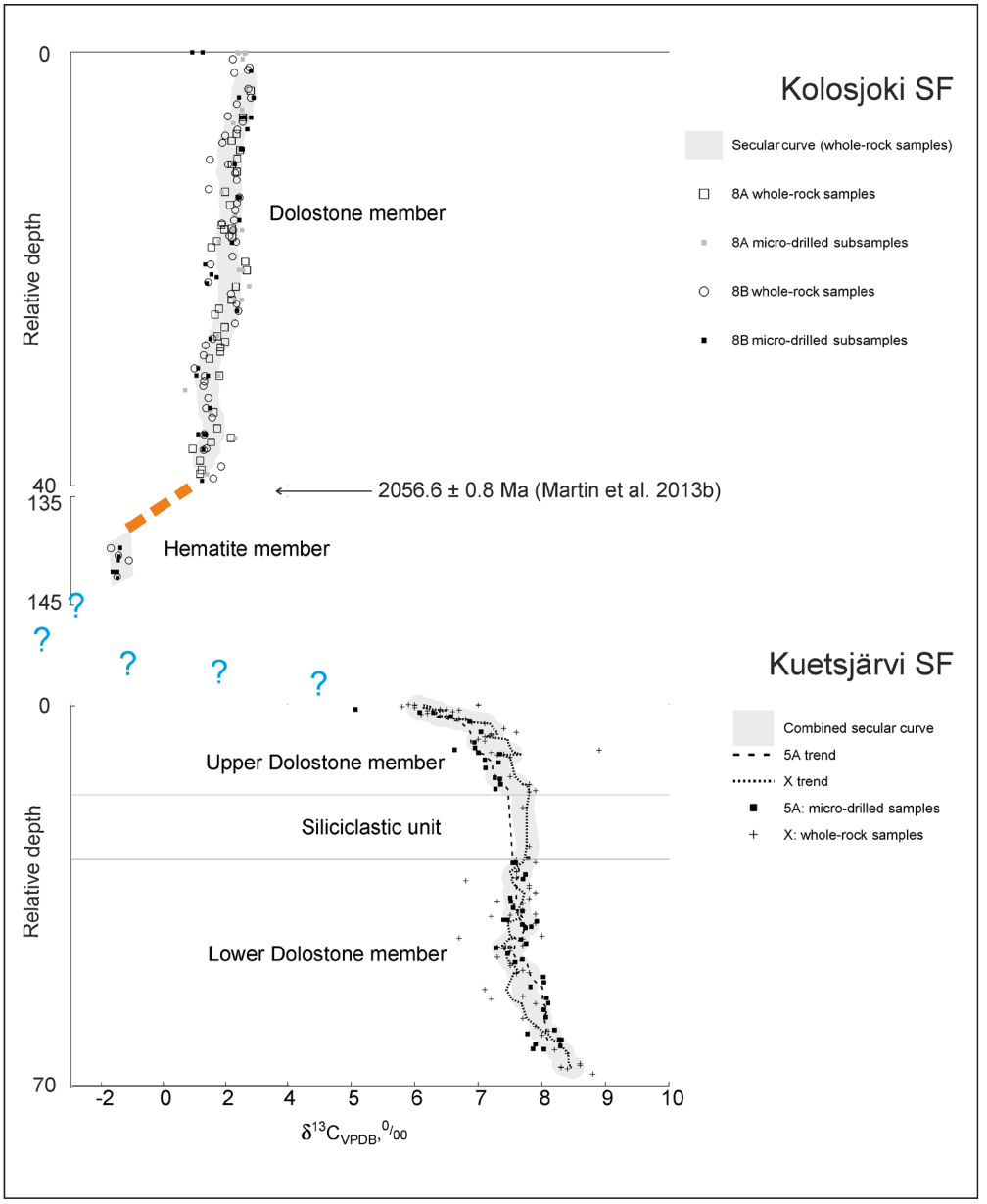

Figure 4. Secular $\delta^{13}C$ curves of the Kuetsjärvi and Kolosjoki sedimentary formations. The secular $\delta^{13}C$ curve of the KuSF is based on the data from Drillcore 5A (Paper I) and Drillcore X (Melezhik et al., 2005b). The secular $\delta^{13}C$ curve of the KoSF is based on data from Drillcores 8A and 8B (Paper II). The question marks represent intervals with no data.

have led to these extremely low $\delta^{13}C$ values (Kump et al., 2011; Paper II).

Préat et al. (2011) investigated the $\delta^{13}C$ evolution of the Lastoursville and Djibalonga subbasins of the FC Formation, the Francevillian Group (Gabon). The investigated sections showed an upwards decreasing trend from high $\delta^{13}C$ values to slightly negative $\delta^{13}C$ values. These trends are the reverse of those found in the KoSF. Thus, the Lastoursville and Djibalonga

subbasins cannot represent time equivalents of the KoSF. They could possibly record a $\delta^{13}C$ trend towards the $\delta^{13}C$ minimum, whereas the KoSF records the minimum and the recovery from it (Paper II).

The $\delta^{13}C$ trend found in the uppermost part of the Nash Fork Formation (the upper Snowy Pass Supergroup, Wyoming Craton) shows some similarities to the $\delta^{13}C$ trends found in Drillcores 8A and 8B (Bekker et al., 2003a).

4.3 The termination of the Lomagundi-Jatuli Isotope Event

The new results from the Kuetsjärvi and Kolosjoki sedimentary formations (Papers I and II) provide new, detailed information about the termination of the LJIE. They provide evidence of (i) decreasing $\delta^{13}C$ values towards the end of the LJIE, and (ii) a $\delta^{13}C$ minimum after the LJIE before 2057 Ma, followed by (iii) an increasing $\delta^{13}C$ trend at 2057 Ma.

The constructed secular $\delta^{13}C$ curve of the KuSF was interpreted to represent the final part of the LJIE (Paper I). Based on the world-wide correlation, the obtained $\delta^{13}C$ curve of the KuSF is clearly concordant with the global $\delta^{13}C$ evolutionary trend and records a partial shift towards normal marine $\delta^{13}C$ values (0-1‰) of sedimentary carbonate rocks (Paper I, Melezhik et al., 2005b). However, the decrease in $\delta^{13}C$ values at the end of LJIE did not apparently stop at normal $\delta^{13}C$ values, but continued to negative $\delta^{13}C$ values. The magnitude of this shift still remains to be resolved. Kump et al. (2011) provide evidence for a greater negative $\delta^{13}C$ shift than the one found in the KoSF (Paper II). The $\delta^{13}C$ data from the KoSF also records a small increase in $\delta^{13}C$ after the negative $\delta^{13}C$ shift (Paper II).

Karhu and Holland (1996) produced a Paleoproterozoic $\delta^{13}C$ curve based on a compilation of previously published results. They recognized an almost 10‰ increase in $\delta^{13}C$ values before ca. 2200 Ma and a decrease of similar magnitude at ca. 2100 Ma. Melezhik et al. (2013b) provided an updated version of the Paleoproterozoic $\delta^{13}C$ curve. According to their compilation, the increasing trend in the $\delta^{13}C$ values may have already started at ca. 2300 Ma. However, that compilation also showed a decrease in $\delta^{13}C$ values around 2100 Ma, a $\delta^{13}C$ minimum around 2000 Ma and a subtle increase in $\delta^{13}C$ following that minimum. The new results from the KoSF provide new evidence for the existence of a distinct $\delta^{13}C$ minimum before 2057 Ma, as well as on an increasing $\delta^{13}C$ trend following it. Thus, it seems that there were at least two $\delta^{13}C$ minimums at 2060 – 2000 Ma.

In Figure 5, the secular $\delta^{13}C$ curves of the KuSF and KoSF are compared to the $\delta^{13}C$ compilation of Karhu and Holland (1996). The sedimentation of the KuSF is set between 2100 and 2057 Ma, based on the decreasing $\delta^{13}C$ trend and the depositional age (2056.6 ± 0.8 Ma; Martin et al., 2013b) of the overlying KoSF. At 2057 Ma the secular $\delta^{13}C$ trend was already recovering from the minimum, which extended at least to -2‰ and possibly even to lower values. The new results from the KoSF indicate that the termination of the LJIE was more complex than previously thought.

4.4 Carbonate precipitates (travertines) of the Kuetsjärvi Sedimentary Formation

Drillcore 5A from the Kuetsjärvi Sedimentary Formation includes abundant carbonate precipitates that are not of sedimentary origin. Rather they represent surficial dolomite and carbonates filling cavities and veins. The cavity and vein fills were interpreted as post-depositional precipitates, whereas the surficial dolomite crusts and cements are likely to have been syn-depositional precipitates (Paper III).

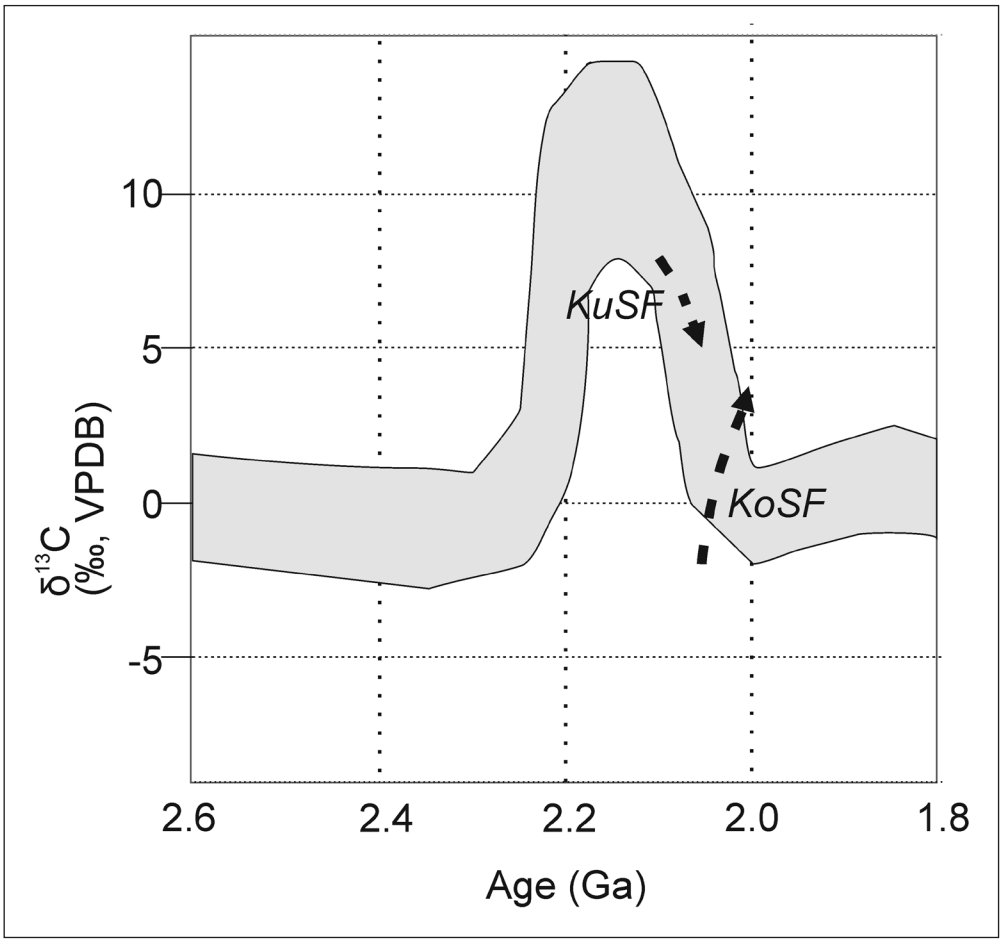

Figure 5. A schematic representation showing the newly obtained $\delta^{13}C_{carb}$ results and the general Paleoproterozoic $\delta^{13}C_{carb}$ curve (sketched from Karhu and Holland, 1996). KuSF = Kuetsjärvi Sedimentary Formation, KoSF = Kolosjoki Sedimentary Formation. The arrows in the figure indicate $\delta^{13}C$ evolution within the KuSF or KoSF.

Drillcore 5A includes abundant small-scale cavities and veins (Paper III). Most of the cavities appear as dissolution cavities. The latest infill of the cavities and veins is usually quartz and/or dolospar. Cavities and veins are walled with rim(s) of sparitic, bladed and/or fibrous, radiating dolomite. In addition to dolomite and quartz, other minor minerals (e.g. calcite, pyrite, talc) are sometimes found in the cavities. White, small-scale stalactites and stalagmites have also been recognized in some cavities. These stalactites have likely formed from dripping water.

Some cavities include dolomite crusts (Paper III). The flooring usually consists of a banded, laminated or massive dolomite crust, which is capped with a thinly-laminated crust. The ceiling of the cavities is sometimes composed of a massive crust underlain by thinly-laminated stalactites, but sometimes there are only stalactites. The thinly-laminated crusts and stalactites are usually composed of gray and white laminae of fibrous (radiating, forming cones) and sparry dolomite. These crusts and stalactites greatly resemble modern travertines (e.g. Jones and Renaut, 2008). In one cavity, the stalactites are composed of gray, white, yellow

and black micritic laminae.

Surficial dolomite crusts (Paper III) are found on bedding and erosional surfaces. These crusts are composed of massive, banded or laminated dolomite. They contain small vugs and veins. Some possible surficial dolomite crusts also include more prominent dissolution cavities (see above). Surficial dolomite rusts are capped with a rim of fibrous/sparry dolomite and a silica sinter or a silcrete layer.

Surficial dolomite cements (Paper III) are found coating uneven surfaces or cementing and corrosively replacing rock fragments. Sometimes these dolomite cements are also filling space between the fragments. Dolomite cements are mainly composed of fibrous dolomite crystals, often with feathery crystal shapes. Similar feathery crystals have been found in travertines (Fouke et al., 2000; Guo and Riding, 1992; Rainey and Jones, 2009).

Compared to their host carbonate rocks, carbonate precipitates generally have lower or similar $\delta^{13}C$ values (Paper III, Fig. 6). The lower $\delta^{13}C$ values suggest an external carbon source. Dolomite crusts (Paper III, Fig. 6) also show higher $\delta^{13}C$ values than the host rocks.

The $\delta^{13}C$ and $\delta^{18}O$ values show moderate positive correlations in the carbonate precipitates (Paper III). Both upwards increasing and decreasing $\delta^{13}C$ and $\delta^{18}O$ trends were found in the dolomite crusts (Paper III). The positive co-variation and the observed trends could be explained by (i) mixing between fluids with different chemical composition (Banner et al., 1988; Banner and Hanson, 1990; Lohmann, 1988), (ii) thermal origin and/or down-flow trends of thermal water (Chafetz et al., 1991; Chafetz and Guidry, 2003; Chafetz and Lawrence, 1994; Friedman, 1970), and/or (iii) evaporation (e.g. Friedman, 1998; Stiller et al., 1985). In some cavities, the $\delta^{13}C$ and $\delta^{18}O$ values show both upward and downward growth from the center (Paper III). These trends in the cavities could perhaps be explained by changing fluid/rock-ratio. Only the contact-altered host carbonates show co-variation between the $\delta^{13}C$ and $\delta^{18}O$ values (Paper I). Thus, the co-variation between the $\delta^{13}C$ and $\delta^{18}O$ values is unlikely to be due to metamorphic alteration.

Melezhik and Fallick (2001) explained the $\delta^{13}C$ and $\delta^{18}O$ trends in the travertines of the KuSF by down-flow trends of hot-spring water possibly associated with evaporation and mixing with the ambient water. This same model could possibly explain the $\delta^{13}C$ and $\delta^{18}O$ trends in the investigated samples from Drillcore 5A (see Paper III).

Carbonate fills, crusts and cements also commonly show higher Mn/Sr ratios (Paper III) than those in the host rocks (Paper I). Higher Mn/Sr ratios are mainly explained by correspondingly higher Mn contents (but relatively similar Sr contents) than those in the host rocks (Papers I and III). The $\delta^{13}C$ and $\delta^{18}O$ values did not generally show co-variation with the Mn/Sr ratios. Therefore, the high Mn/Sr ratios most likely reflect depositional conditions. Perhaps, the high Mn contents reflect the siliceous materials in the samples (Paper III; Pentecost, 2005, pp. 118).

Some carbonate fills and crusts (Paper III) show petrographic similarities to the hot-spring travertines reported by Melezhik and Fallick (2001). However, the new $\delta^{13}C$ results show a relatively narrow compositional variation, whereas travertines are commonly characterized by $\delta^{13}C$ values varying widely from -4 to +8‰. Melezhik and Fallick (2001) and Melezhik et al. (2004) reported $\delta^{13}C$ values from the KuSF that are in accord with these observations. The absence of lower $\delta^{13}C$ values in this study could possibly be explained by e.g. precipitation in distal pools or evaporation, according to the model of Melezhik and Fallick (2001). Moreover,

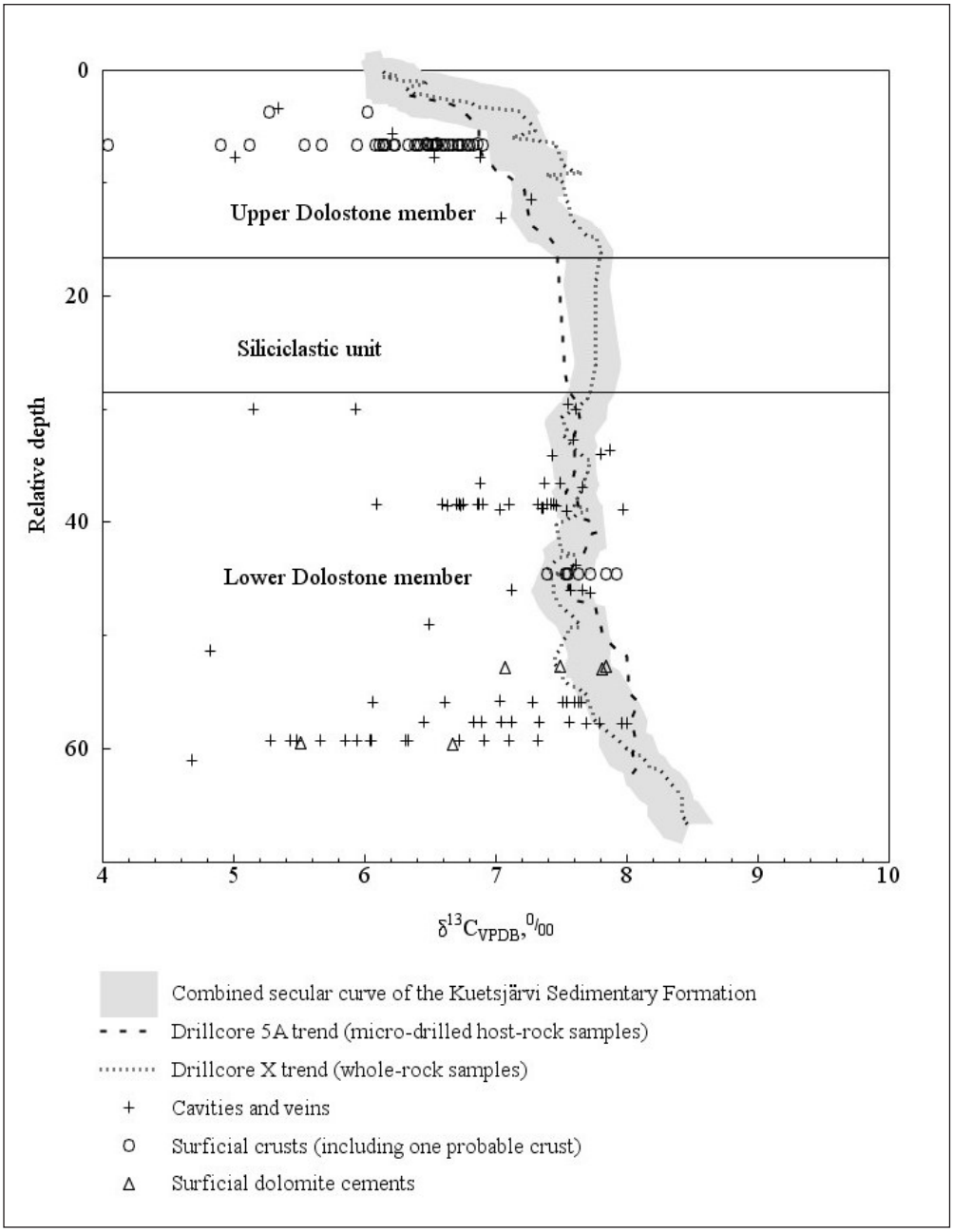

Figure 6. Carbon isotope composition of carbonate precipitates (from Paper III) plotted against the secular $\delta^{13}C$ curve of the Kuetsjärvi Sedimentary Formation. The figure has been modified from Paper I. The data for the host rocks of Drillcore 5A are from Paper I and the data for Drillcore X from Melezhik et al. (2005b).

the host dolostones show high $\delta^{13}C$ values (5 – 8 ‰). Due to dissolution of the host rocks, the travertines of the KuSF could also show higher $\delta^{13}C$ values than those in modern travertines.

In the absence of a terrestrial biosphere, high pCO_2 soils, a common-ion effect caused by dissolution of evaporites (e.g. Calaforra et al. 2008, Wigley, 1973a) or incongruent dissolution of dolomites (e.g. Wigley, 1973b) could each explain the formation of the cavities as well as the precipitation of the carbonate fills, crusts and cements. However, this cannot in itself explain the lower $\delta^{13}C$ values (compared to host rocks) in the investigated samples (see Paper III). Thus, some external carbon source is needed. Moreover, common-ion effect due to dissolution of Ca-rich evaporites (Wigley, 1973a) or dolomites (Wigley, 1973b) results in precipitation of calcite prior to dolomite. Calcite is only a minor constituent in Drillcore 5A and there is no indication of dolomitization. A common-ion effect due to dissolution of Mg-rich evaporites could possibly explain the precipitation of the dolomitic carbonate fills, crusts and cements, but no pseudomorphs or relicts of Mg-rich evaporites have been found in the KuSF.

Atmospheric/meteoric (ambient or heated) water cannot independently precipitate carbonates under a high pCO_2 atmosphere (see Brasier, 2011). Degassing from meteoric water could have been possible due to common-ion effect (as described above), under an ice-cover or from freezing water. However, there is no textural or sedimentological indication for the latter processes (Paper III). Moreover, evaporation alone cannot explain upwards decreasing $\delta^{13}C$ trends in the crusts (see Paper III).

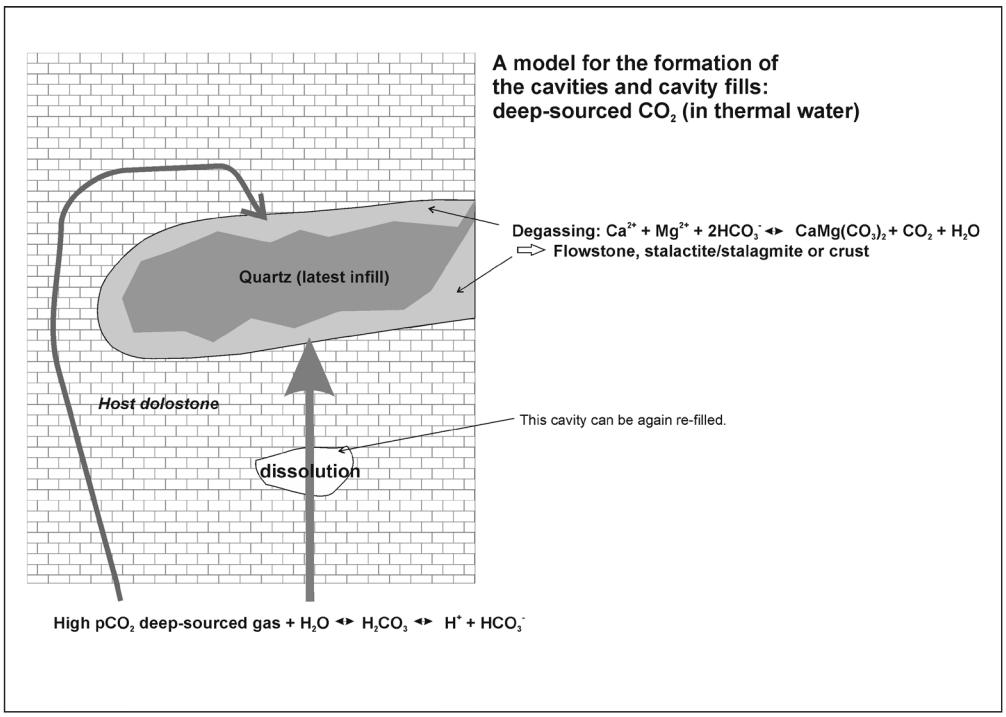

Figure 7. A schematic representation of the model explaining the formation of cavities and cavity fills due to activity of deep-sourced CO_2 (modified from Brasier, 2011).

Thus, the most likely explanation (see Paper III) for the formation of the cavities and the carbonate fills, crusts and cements is deep-sourced CO_2, likely as thermal water (Fig. 7) (e.g. Duliński et al., 1995; Pentecost and Viles, 1994; Yoshimura et al., 2004). Deep-sourced fluid could be volcanic or produced by metamorphic reactions. Degassing might also have happened due to boiling (e.g. Arnósson, 1989), although temperatures well below the boiling point can precipitate travertines today (e.g. Fouke et al., 2000). Nevertheless, boiling solely could not explain all observed $\delta^{13}C$ trends.

The investigated precipitates in the KuSF are interpreted as thermal travertines. The new results indicate that these travertines have formed both post-depositionally and syn-depositionally. The cavity and vein fills and the surficial precipitates likely have the same origin. Precambrian (thermal) travertines have not been widely reported – thus the KuSF is a unique locality. Travertine precipitation likely indicates occasional subaerial exposure in the KuSF (see e.g. Melezhik and Fallick, 2001).

There have been attempts to explain the extreme ^{13}C enrichment during the LJIE in terms of local factors, e.g. evaporation in hypersaline environments (e.g. Friedman, 1998; Stiller et al., 1985) and hot-spring activity (e.g. Friedman, 1970). The Kuetsjärvi Sedimentary Formation (extremely enriched in ^{13}C) was likely deposited in an environment, where both evaporation processes and hot-springs were acting. Lower $\delta^{13}C$ values were commonly found in the carbonate fills, crusts and cements compared to their host rocks (Papers I, III). If the host rocks had been affected by the precipitation of carbonate fills, crusts and cements, negative peaks in the $\delta^{13}C$ trend should have been found. However, the $\delta^{13}C$ values of the host dolostones and limestones do not show co-variation with the abundance of the carbonate fills, crusts and cements (Paper I). Moreover, similar $\delta^{13}C$ curves were found in two cores situated 25 km apart (Paper I). Local factors, such as evaporation or hot-springs, would be unlikely to cause such similar $\delta^{13}C$ trends in these two cores.

4.5 Future research

The results from the Kuetsjärvi Sedimentary Formation seem to be in good agreement with previously published reconstructions of the Paleoproterozoic $\delta^{13}C$ curve. However, the reasons for the ^{13}C enrichment in the sedimentary carbonates deposited during the LJIE still remains unclear.

The $\delta^{13}C$ minimum after the LJIE has only been documented in a few localities, so that the magnitude of this minimum in the global context is not yet well constrained. It also seems that there were at least two $\delta^{13}C$ minimums at ca. 2060 – 2000 Ma. More research is needed on sedimentary carbonates coeval with the Kolosjoki Sedimentary Formation. One good target would be the Il´mozero Formation in the NW Russia, with a depositional age closely corresponding to that of the KoSF.

Carbonate precipitates in the KuSF apparently represent thermal travertines. Deep-sourced CO_2 was most likely contributing in their precipitation. The KuSF is one of the rare Precambrian localities where travertines have been found. More research is needed in order to understand the formation of cavities and cavity fills in environments where the terrestrial biosphere and soils high in CO_2 are missing.

5 Concluding remarks

New evidence is provided for (i) the decreasing $\delta^{13}C$ trend at the end of the LJIE, (ii) a $\delta^{13}C$ minimum after the LJIE, followed by (iii) an increasing $\delta^{13}C$ trend.

New and previously obtained $\delta^{13}C$ data

were used to construct a secular $\delta^{13}C$ curve for the KuSF. This $\delta^{13}C$ curve shows an upwards decreasing stratigraphic trend from ca. 8 to 5‰. Similarities with $\delta^{13}C$ trends in other localities world-wide were found. The $\delta^{13}C$ curve of the KuSF was interpreted to represent the latest part of the LJIE. Separate cores from the KuSF yielded similar secular $\delta^{13}C$ curves, interpreted to reflect a global signal.

The $\delta^{13}C$ data from two newly investigated drillcores were used to construct a secular $\delta^{13}C$ curve for the KoSF. This curve starts from low $\delta^{13}C$ values (down to -2‰), indicating the existence of a $\delta^{13}C$ minimum in the curve before 2057 Ma. This was followed by a subtle increase in $\delta^{13}C$ (up to 3‰).

The investigated drillcore from the KuSF includes abundant small-scale cavities, veins, surficial dolomite crusts and surficial dolomite cements. The carbonate fills, crusts and cements commonly show lower $\delta^{13}C$ values than those in the host rocks. The carbonate fills, crusts and cements have probably been precipitated from deep-sourced thermal fluids. The investigated precipitates were interpreted as travertine and "cave travertine". The KuSF is apparently one of the rare Precambrian localities from which travertines have been described. Local surficial crusts and subaerial cavity fills indicate periodic exposure of the KuSF during and after its deposition.

References

Amelin, Yu.V., Heaman, L.M., Semenov, V.S., 1995. U–Pb geochronology of layered mafic intrusions in the eastern Baltic Shield: implications for the timing and duration of Paleoproterozoic continental rifting. Precambrian Research 75, 31–46.

Anderson, T.F., Arthur, M.A., 1983. Stable isotopes of oxygen and carbon and their application to sedimentologic and paleoenvironmental problems, in: Arthur, M.A., Anderson, T.F., Kaplan, I.R., Veizer, J., Land, L.S. (Eds.), Stable Isotopes in Sedimentary Geology, Volume 10, Columbia SC: SEPM Short Course. Chapter 1.

Arnórsson, S., 1989. Deposition of calcium carbonate minerals from geothermal waters – theoretical considerations. Geothermics 18, 33–39.

Aspler, L.B., Chiarenzelli, J.R., 1998. Two Neoarchean supercontinents? Evidence from the Paleoproterozoic. Sedimentary Geology 120, 75–104.

Baker, A.J., Fallick, A.E., 1989a. Evidence from Lewisian limestones for isotopically heavy carbon in two-thousand-million-year-old sea water. Nature 337, 352–354.

Baker, A.J., Fallick, A.E., 1989b. Heavy carbon in two-billion-year-old marbles from Lofoten-Vesterålen, Norway: implications for the Precambrian carbon cycle. Geochimica et Cosmochimica Acta 53, 1111–1115.

Banner, J.L., Hanson, G.N., 1990. Calculation of simultaneous isotopic and trace element variations during water–rock interaction with applications to carbonate diagenesis. Geochimica et Cosmochimica Acta, 54, 3123–3137.

Banner, J.L., Hanson, G.N. and Meyers, W.J., 1988. Water–rock interaction history of regionally extensive dolomites of the Burlington-Keokuk Formation (Mississippian): isotopic evidence, in: Shukla, V., Baker, P.A. (Edit.), Sedimentology and Geochemistry of Dolostones. SEPM Special Publication 43, 97–113.

Bein, A., 1986. Stable isotopes, iron and phosphorus in a sequence of lacustrine carbonates–paleolimnic implications. Chemical Geology (Isotope Geoscience Section) 4, 305–313.

Bekker, A., Holland, H.D., Wang, P.-L., Rumble III, D., Stein, H.J., Hannah, J.L., Coetzee, L.L., Beukes, N.J., 2004. Dating the rise of atmospheric oxygen. Nature 427, 117–120.

Bekker, A., Holland, H.D., 2012. Oxygen overshoot and recovery during the early Paleoproterozoic. Earth and Planetary Science Letters 317–318, 295–304.

Bekker, A., Holmden, C., Beukes, N.J., Kenig, F., Eglington, B., Patterson, W.P., 2008. Fractionation between inorganic and organic carbon during the Lomagundi (2.22–2.1 Ga) carbon isotope excursion. Earth and Planetary Science Letters 271, 278–291.

Bekker, A., Karhu, J.A, Eriksson, K.A., Kaufman, A.J., 2003a. Chemostratigraphy of Paleoproteroizoic carbonate successions of the Wyoming Craton: tectonic forcing of biogeochemical change? Precambrian Research 120, 279–325.

Bekker, A., Karhu, J.A., Kaufman, A.J., 2006. Carbon isotope record for the onset of the Lomagundi carbon isotope excursion in the Great Lakes area, North America. Precambrian Research 148, 145–180.

Bekker, A., Kaufman, A.J., Karhu, J.A., Beukes,

N.J., Swart, Q.D., Coetzee, L.L., Eriksson, K.A., 2001. Chemostratigraphy of the Paleoproterozoic Duitschland Formation, South Africa: implications for coupled climate change and carbon cycling. American Journal of Science 301, 261–285.

Bekker, A., Kaufman, A.J., Karhu, J.A., Eriksson, K.A., 2005. Evidence for Paleoproterozoic cap carbonates in North America. Precambrian Research 137, 167–206.

Bekker, A., Sial, A.N., Karhu, J.A., Ferreira, V.P., Noce, C.M., Kaufman, A.J., Romano, A.W., Pimentel, M.M., 2003b. Chemostratigraphy of carbonates from the Minas Supergroup, Quadrilátero Ferrífero (Iron Quadrangle), Brazil: a stratigraphic record of Early Proterozoic atmospheric, biogeochemical and climatic change. American Journal of Science 303, 865–904.

Berthelsen, A., Marker, M., 1986. Tectonics of the Kola collision suture and adjacent Archaen and Early Proterozoic terrains in the northeastern region of the Baltic Shield. Tectonophysics 126, 31–55.

Botz, R., Stoffers, P., Faber, E., Tietze, K., 1988. Isotope geochemistry of carbonate sediments from Lake Kivu (East–Central Africa). Chemical Geology 69, 299–308.

Brasier, A.T., 2011. Searching for travertines, calcretes and speleothems in deep time: Processes, appearances, predictions and the impact of plants. Earth-Science Reviews 104, 213–239.

Brocks, J.J., Logan, G.A., Buick, R., Summons, R.E., 1999. Archean Molecular Fossils and the Early Rise of Eukaryotes. Science 285, 1033–1036.

Broecker, W.S., 1970. A boundary condition on the evolution of atmospheric oxygen. Journal of Geophysical Research 75, 3553–3557.

Buick, I.S., Uken, R., Gibson, R.L., Wallmach, T., 1998. High-$\delta^{13}C$ Paleoproterozoic carbonates from the Transvaal Supergroup, South Africa. Geology 26, 875–878.

Burne, R.V., Moore, L.S., 1987. Microbialites: organosedimentary deposits of benthic microbial communities. PALAIOS 2, 241–254.

Calaforra, J., Forti, P., Fernandez-Cortes, A., 2008. Speleothems in gypsum caves and their paleoclimatological significance. Environmental Geology 53, 1099–1105.

Campbell, I. H., & Squire, R. J., 2010. The mountains that triggered the Late Neoproterozoic increase in oxygen: the Second Great Oxidation Event. Geochimica et Cosmochimica Acta 74, 4187–4206.

Canfield, D.E., 1998. A new model for Proterozoic ocean chemistry. Nature 396, 450–453.

Canfield, D.E., 2005. The early history of atmospheric oxygen: homage to Robert A. Garrels. Annual Review of Earth and Planteary Sciences 33, 1–36.

Catling, D.C., Zahnle, K.J., McKay, C.P., 2001. Biogenic Methane, Hydrogen Escape, and the Irreversible Oxidation of Early Earth. Science 293, 839–843.

Chafetz, H.S., Guidry, S.A., 2003. Deposition and diagenesis of Mammoth Hot Spring travertine, Yellowstone National Park, Wyoming, USA. Canadian Journal of Earth Sciences 40, 1515–1529.

Chafetz, H.S., Lawrence, J.R., 1994. Stable isotopic variability within modern travertines. Géographie physique et Quaternaire 48, 257–273.

Chafetz, H.S., Rush, P.F., Utech, N.M., 1991. Microenvironmental controls on mineralogy and habit of $CaCO_3$ precipitates: an example from an active travertine system. Sedimentology 38, 107–126.

Chandler, F.W., 1980. Proterozoic redbed sequences of Canada. Canadian Geological Survey Bulletin 311, 53 pp.

Claire, M.W., Catling, D.C., Zahnle, K.J., 2006. Biogeochemical modeling of the rise in atmospheric oxygen. Geobiology 4, 239–269.

Cloud Jr, P.E., 1968. Atmospheric and hydrospheric evolution on the primitive Earth. Science 160, 729–736.

Condie, K.C., Des Marais, D.J., Abbot, D., 2001. Precambrian superplumes and supercontinents: a record in black shales, carbon isotopes, and paleoclimates? Precambrian Research 106, 239–260.

Condie, K.C., O´Neill C., Aster, R.C., 2009. Evidence and implications for a widespread magmatic shutdown for 250 My on Earth. Earth and Planetary Science Letters 282, 294–298.

Corbella, M., Ayora, C., Cardellach, E., 2004. Hydrothermal mixing, carbonate dissolution and sulfide precipitation in Mississippi Valley-type deposits. Mineralium Deposita 39, 344–357.

Deines, P. 2002. The carbon isotope geochemistry of mantle xenoliths. Earth Science Reviews 58, 247–278.

Des Marais, D.J., Bauld, J., Palmisano, A.C., Summons, R.E., Ward, D.M., 1992a. The biochemistry of carbon in modern microbial mats, in: Schopf, J.W., Klein, C. (Eds.), The Proterozoic Biosphere. Cambridge University Press, Cambridge, pp. 299–308.

Des Marais, D.J., Strauss, H., Summons, R. E., Hayes, J.M., 1992b. Carbon isotope evidence for the stepwise oxidation of the Proterozoic environment. Nature 359, 605–609.

Des Marais, D.J., 2001. Isotopic Evolution of the Biogeochemical Carbon Cycle During the Precambrian, in: Valley, J.W.. Cole, D.R. (Eds.), Stable Isotope Geochemistry. Reviews in Mineralogy and Geochemistry, Volume 43. Mineralogical Society of America, Geochemical Society, Washington D.C., pp. 555–578.

Dickens, G.R., O´Neil, J.R., Rea, D.K., Owen, R.M., 1995. Dissociation of oceanic methane hydrate as

a cause of the carbon isotope excursion at the end of the Paleocene. Paleoceanography 10, 965–971.
Djidi K., Bakalowicz, M., Benali, A.M., 2008. Mixed, classical and hydrothermal karstification in a carbonate aquifer: Hydrogeological consequences. The case of the Saida aquifer system, Algeria. Comptes Rendus Geoscience 340, 462–473.
Dublyansky, Y.V., 1995. Speleogenetic history of the Hungarian hydrothermal karst. Environmental Geology 25, 24–35.
Duliński, M., Grabczak, J., Kostecka, A., Weclawik, S., 1995. Stable isotope composition of spelean calcites and gaseous CO_2 from Tylicz (Polish Carpathians). Chemical Geology 125, 271–280.
Emrich, K., Enhalt, D.H., Vogel, J.C. 1970. Carbon isotope fractionation during the precipitation of calcium carbonate. Earth and Planetary Science Letters 8, 363–371.
Evans, D.A.D., 2003. A fundamental Precambrian-Phanerozoic shift in Earth's glacial style? Tectonophysics 375, 353–385.
Evans, D.A., Beukes, N.J., Kirschvink, J.L., 1997. Low-latitude glaciation in the Palaeproterozoic era. Nature 386, 263–266.
Fairchild, I.J., Borsato, A., Tooth, A.F., Frisia, S., Hawkesworth, C.J., Huang, Y., McDermott, F., Spiro, B., 2000. Controls on trace element (Sr-Mg) compositions of carbonate cave waters: implications for speleothem climatic records. Chemical Geology 166, 255–269.
Farquhar, J., Bao, H. M., Thiemens, M., 2000. Atmospheric influence of Earth's earliest sulfur cycle. Science 289, 756–758.
Ford, T.F., Pedley, H.M., 1996. A review of tufa and travertine deposits of the world. Earth-Science Reviews 41, 117–175.
Ford, D.F., Williams, P., 2007. Karst Hydrogeology and Geomorphology. John Wiley & Sons, Ltd, West Sussex, England, 562 p.
Fouke, B.W., Farmer, J.D., Des Marais, D.J., Pratt L., Sturchio, N.C., Burns, P.C., Discipulo, M.K., 2000. Depositinal facies and aqueous-solid geochemistry of travertine-depositing hot springs (Angel Terrace, Mammoth Hot Springs, Yellowstone National Park, USA). Journal of Sedimentary Research 70, 565–585.
Friedman, I., 1970. Some investigations of deposition of travertine from Hot Springs–I. The isotopic chemistry of a travertine-depositing spring. Geochimica et Cosmochimica Acta 34, 1303–1315.
Friedman, G.M., 1998. Temperature and salinity effects on ^{18}O fractionation of rapidly precipitated carbonates: laboratory experiments with alkaline lake water – perspective. Episodes 21, 97–98.
Galimov, E.M., Kuznetsova, N.G., Prokhorov, V.S., 1968. On the problem of the Earth's ancient atmosphere composition in connection with results of isotope analysis of carbon from the Precambrian carbonates. Geochemistry 11, 1376–1381 (In Russian with an English abstract).
Gaucher, C., Sial, A.N., Ferreira, V.P., Pimentel, M.M., Chiglino, L., Sprechmann, P., 2007. Chemostratigraphy of the Cerro Victoria Formation (Lower Cambrian, Uruguay): evidence for progressive climate stabilization across the Precambrian–Cambrian boundary. Chemical Geology 237, 28–46.
Gauthier-Lafaye, F., Weber, F., 2003. Natural nuclear fission reactors: time constraints for occurrence, and their relation to uranium and manganese deposits and to evolution of the atmosphere. Precambrian Research 120, 81–100.
Guo, L., Riding, R., 1992. Aragonite laminae in hot water travertine crusts, Rapolano Terme, Italy. Sedimentology 39, 1067–1079.
Guo, Q., Strauss, H., Kaufman, A.J., Schröder, S., Gutzmer, J., Wing, B., Baker, M.A., Bekker, A., Kim, S.-T., Farquhar, J., 2009. Reconstructing Earth´s surface oxidation across the Archean-Proterozoic transition. Geology 37, 399–402.
Han, T-M., Runnegar, B., 1992. Megascopic Eukaryotic Algae from the 2.1-Billion-Year-Old Negaunee Iron-Formation, Michigan. Science 257, 232–235.
Hanski, E.J., Huhma, H., Smolkin, V.F., Vaasjoki, M., 1990. The age of ferropicritic volcanics and comagmatic Ni-bearing intrusions at Pechenga, Kola Peninsula, U.S.S.R. Geological Society of Finland Bulletin 62, 123–133.
Haq, B.U., 1998. Gas Hydrates: Greenhouse Nightmare? Energy Panacea or Pipe Dream? GSA Today 8, 2–6.
Holland, H. D., 1992. Distribution and paleoenvironmental interpretation of Proterozoic paleosols, in: J. W. Schopf & C. Klein (Eds.), The Proterozoic Biosphere, A Multidisciplinary Study. Cambridge University Press, New York, pp. 153–155.
Holland, H.D., 2002. Volcanic gases, black smokers, and the Great Oxidation Event. Geochimica et Cosmochimica Acta 66, 3811–3826.
Holland, H. D., 2006. The oxygenation of the atmosphere and oceans. Philosophical Transactions of the Royal Society B 361, 903–915.
Holland, H. D., 2009. Why the atmosphere became oxygenated: a proposal. Geochimica et Cosmochimica Acta 73, 5241–5255.
Holland, H.D., Lazar, B., McGaffrey, M., 1986. Evolution of the atmosphere and oceans. Nature 320, 27–33.
Hollander, D.J., McKenzie, J.A., 1991. CO_2 control on carbon-isotope fractionation during aqueous photosynthesis: a paleo-pCO_2 barometer. Geology 19, 929–932.
Holser, W.T., Schidlowski, M., Mackenzie, F.T., Maynard, J.B., 1988. Geochemical cycles of carbon and sulphur, in: Gregor, C.B., Garrels,

R.M., Mackenzie, F.T., Maynard, J.B. (Eds.), Chemical Cycles in the Evolution of the Earth. John Wiley & Sons, New York, pp. 105–173.

Hudson, J.D., 1977. Stable isotopes and limestone lithification. Journal of the Geological Society London133, 637–660.

Irwin, H., Curtis, C., Coleman, M., 1977. Isotopic evidence for source of diagenetic carbonates formed during burial of organic-rich sediments. Nature 260, 209–213.

Jenkyns, H.C., 1988. The early Toarcian (Jurassic) anoxic event: Stratigraphic, sedimentary, and geochemical evidence. American Journal of Science 288, 101–151.

Jones, B., Renaut, R.W., 2008. Cyclic development of large, complex, calcite dendrite crystals in the Clinton travertine, Interior British Columbia, Canada. Sedimentary Geology 203, 17–35.

Karhu, J.A., 1993. Paleoproterozoic evolution of the carbon isotope ratios of sedimentary carbonates in the Fennoscandian Shield. Geological Survey of Finland Bulletin 371, 1–87.

Karhu, J.A., Holland, H.D., 1996. Carbon isotopes and the rise of atmospheric oxygen. Geology 24, 867–879.

Karhu, J., Kortelainen, N.M., Huhma, H., Perttunen, V., Sergeev, S., 2008. The end of the Paleoproterozoic carbon isotope excursion; new time constraints (electronic resource). In: 33rd International Geological Congress, Oslo, Norway, August 6–14, 2008, Abstract CD-ROM, 1 p., Optical disc (CD-ROM).

Karhu, J.A., Melezhik, V.A., 1992. Carbon isotope systematics of early Proterozoic sedimentary carbonates in the Kola Peninsula, Russia: correlations with Jatulian formations in Karelia, in: Balagansky, V.V., Mitrofanov, F.P. (Eds.), Correlation of Precambrian Formation of the Kola-Karelia Region and Finland. Kola Scientific Centre of the Russian Academy of Sciences, Apatity, pp. 48–53.

Kasting, J. F., 1987. Theoretical constraints on oxygen and carbon dioxide concentrations in the Precambrian atmosphere. Precambrian Research 34, 205–229.

Kasting J.F, 1988. Runaway and moist greenhouse atmospheres and the evolution of Earth and Venus. Icarus 74, 472–494.

Kasting, J.F., Eggler, D.H., Raeburn, S.P., 1993. Mantle Redox Evolution and the Oxidation State of the Archean atmosphere. The Journal of Geology 101, 245–257

Kaufman, A.J., Knoll, A.H., 1995. Neoproterozoic variations in the C-isotopic composition of seawater: stratigraphic and biogeochemical implications. Precambrian Research 73, 27-49.

Keith, M.L., Weber, J.N., 1964. Carbon and oxygen isotopic composition of selected limestones and fossils. Geochimica et Cosmochimica Acta 28, 1787–1816.

Kopp, R.E., Kirschvink, J.L., Hilburn, I.A., Nash, C.Z., 2005. The Paleoproterozoic snowball Earth: a climate disaster triggered by the evolution of oxygenic photosynthesis. Proceedings of the National Academy of Sciences of the United States of America 102, 11131–11136.

Kump, L.R., Barley, M.E., 2007. Increased subaerial volcanism and the rise of atmospheric oxygen 2.5 billion years ago. Nature 448, 1033-1036.

Kump, L.R., Fallick, A.E., Melezhik, V.A. Strauss, H., Lepland, A., 2013. The Great Oxidation Event, in: Melezhik, V.A., Kump, L.R., Fallick, A.E., Strauss, H., Hanski, E.J., Prave, A.R., Lepland, A. (Eds.), Reading the Archive of Earth´s Oxygenation, Volume 3: Global Events and the Fennoscandian Arctic Russia – Drilling Early Earth Project. Springer-Verlag, Berlin Heidelberg. Chapter 8.1, pp. 1517–1523.

Kump, L.R., Junium, C., Arthur, M.A., Brasier, A., Fallick, A., Melezhik, V., Lepland, A., Črne .A.E., Luo, G., 2011. Isotopic Evidence for Massive Oxidation of Organic Matter Following the Great Oxidation Event. Science 334, 1694–1696.

Kump, L.R., Kasting, J.F., Barley, M.E., 2001. Rise of atmospheric oxygen and the "upside-down" Archean mantle. Geochemistry Geophysics Geosystems 2, paper number 2000GC000114.

Kvenvolden, K.A., 1993. Gas hydrates – Geological perspective and global change. Reviews of Geophysics 3, 173–187.

Kvenvolden, K.A., 1999. Potential effects of gas hydrate on humal welfare. Proceedings of the National Academy of Sciences of the United States of America 96, 3420-3426. Colloquium Paper.

Lindsay, J.F., Brasier, M.D., 2002. Did global tectonics drive early biosphere evolution? Carbon isotope record from 2.6 to 1.9 Ga carbonates of Western Australian basins. Precambrian Research 114, 1–34.

Lohmann, K.C., 1988. Geochemical patterns of meteoric diagenesis systems and their application to studies of paleokarst, in: James, N.P., Choquette, P.W. (Ed.), Paleokarst. Springer-Verlag, New York, pp.58–80.

Maheshwari, A., Sial, A.N., Chittora, V.K., 1999. High-$\delta^{13}C$ Paleoproterozoic Carbonates from the Aravalli Supergroup, Western India. International Geology Review 41, 949–954.

Maheshwari, A., Sial, A.N., Gaucher, C., Bossi, J., Bekker, A., Ferreira, V.P., Romano A.W., 2010. Global nature of the Paleoproterozoic Lomagundi carbon isotope excursion: A review of occurrences in Brazil, India and Uruguay. Precambrian Research 182, 274–299.

Martin, A.P., Condon, D.J., Prave, A.R., Lepland, A., 2013a. A review of temporal constraints for the Paleoproterozoic large, positive carbonate carbon

isotope excursion (the Lomagundi-Jatuli Event). Eart-Science Reviews 127, 242–261.

Martin, A.P., Condon, D.J., Prave, A.R., Melezhik, V.A., Lepland, A., Fallick, A.E., 2013b. Dating the termination of the Palaeoproterozoic Lomagundi-Jatuli carbon isotopic event in the North Transfennoscandian Greenstone Belt. Precambrian Research 224, 160–168.

Melezhik, V.A., Fallick, A.E., 1996. A widespread positive $\delta^{13}C_{carb}$ anomaly at around 2.33–2.06 Ga on the Fennoscandian Shield: a paradox? Terra Nova 8, 141–157.

Melezhik, V.A., Fallick, A.E., 2001. Palaeoproterozoic travertines of volcanic affiliation from a ^{13}C-rich rift lake environment. Chemical Geology 173, 293–312.

Melezhik, V.A., Fallick, A.E., 2003. $\delta^{13}C$ and $\delta^{18}O$ variations in primary and secondary carbonates: several contrasting examples from Palaeoproterozoic ^{13}C-rich metamorphosed dolostones. Chemical Geology 201, 213–228.

Melezhik, V.A., Fallick, A.E., 2005. Palaeoproterozoic, rift-related, ^{13}C-rich, lacustrine carbonates, NW Russia. Part I: Sedimentology and major element geochemistry. Transactions of the Royal Society of Edinburgh: Earth Sciences 95, 393–421.

Melezhik, V.A., Fallick, A.E., 2010. On the Lomagundi-Jatuli carbon isotopic event: the evidence from the Kalix Greenstone Belt, Sweden. Precambrian Research 179, 165–190.

Melezhik, V.A., Fallick, A.E., Clark, T., 1997. Two billion year old isotopically heavy carbon: evidence from the Labrador Trough, Canada. Canadian Journal of Earth Sciences 34, 271–285.

Melezhik, V.A., Fallick, A.E., Filippov, M.M., Larsen, O. 1999a. Karelian shungite – an indication of 2.0-Ga-old metamorphosed oil-shale and generation of petroleum: geology, lithology and geochemistry. Earth-Science Reviews 47, 1–40.

Melezhik, V.A., Fallick, A.E., Grillo, S.M., 2004a. Subaerial exposure surfaces in a Palaeoproteroizoic ^{13}C-rich dolostone sequence from the Pechenga Greenstone Belt: palaeoenvironmental and isotopic implications for the 2330-2060 Ma global isotope excursion of $^{13}C/^{12}C$. Precambrian Research 133, 75–103.

Melezhik, V.A., Fallick, A.E., Hanski, E., Kump, L., Lepland, A., Prave, A., Strauss, H., 2005a. Emergence of the aereobic biosphere during the Archean-Proterozoic transition: challenges for future research. GSA Today 15, 4–11.

Melezhik, V.A., Fallick, A.E., Kuznetsov, A.B., 2005b. Palaeoproterozoic, rift-related, ^{13}C-rich, lacustrine carbonates, NW Russia. Part II: Global isotope signal recorded in the lacustrine dolostones. Transactions of the Royal Society of Edinburgh: Earth Sciences 95, 423–444.

Melezhik, V.A., Fallick, A.E., Martin, A.P., Condon, D.J., Kump, L.R., Brasier A.T., Salminen P.E., 2013a. The Palaeoproterozoic Perturbation of the Global Carbon Cycle: The Lomagundi-Jatuli Isotopic Event, in: Melezhik, V.A., Kump L.R., Fallick, A.E., Strauss, H., Hanski, E.J., Prave, A.R., Lepland, A (Eds.), Reading the Archive of Earth's Oxygenation, Volume 3: Global Events and the Fennoscandian Arctic Russia – Drilling Early Earth Project. Springer-Verlag, Berlin-Heidelberg. Chapter 7.3, pp. 1111–1150.

Melezhik, V.A., Fallick, A.E., Medvedev, P.V., Makarikhin, V.V., 1999b. Extreme $^{13}Ccarb$ enrichment in ca. 2.0 Ga magnesite-stromatolite-dolomite-'red beds' association in a global context: a case for the world-wide signal enhanced by a local environment. Earth-Science Reviews 48, 71–120.

Melezhik, V.A., Fallick, A.E., Rychanchik, D.V., Kuznetsov, A.B., 2005c. Palaeoproterozoic evaporites in Fennoscandia: implications for seawater sulphate, the rise of atmospheric oxygen and local amplification of the $\delta^{13}C$ excursion. Terra Nova 17, 141–148.

Melezhik, V.A., Fallick, A.E., Smirnov, Yu.P., Yakovlev, Yu.N., 2003. Fractionation of carbon and oxygen isotopes in ^{13}C-rich Palaeoproterozoic dolostones in the transition from medium-grade to high-grade greenschist facies: a case study from the Kola Superdeep Drillhole. Journal of the Geological Society, London 160, 71–82.

Melezhik, V.A., Filippov, M.M., Romashkin, A.E., 2004b. A giant Palaeoproterozoic deposit of shungite in NW Russia: genesis and practical applications. Ore Geology Reviews 24, 135–154.

Melezhik, V.A., Hanski, E.J., 2013. The Pechenga Greenstone Belt, in: Melezhik, V.A., Prave, A.R., Hanski, E.J., Fallick, A.E., Lepland, A., R. Kump, L.R. Strauss, H. (Eds.), Reading the Archive of Earth's Oxygenation, Volume 1: The Palaeoproterozoic of Fennoscandia as Context for the Fennoscandian Arctic Russia - Drilling Earth Project. Springer-Verlag, Berlin-Heidelberg. Chapter 4.2, pp. 289–385.

Melezhik, V.A., Huhma, H., Condon, D.J., Fallick, A.E., Whitehouse, M.J., 2007. Temporal constraints on the Paleoproterozoic Lomagundi-Jatuli carbon isotopic event. Geology 35, 655–658.

Melezhik, V.A., Lepland, A., 2006. ICDP Workshop on the Emerging Modern Aerobic Earth System. Scientific Drilling 2, 56–57.

Melezhik, V.A., Prave, A.R., Lepland, A., Hanski, E.J., Romsahkin, A.E., Rychanchik, D.V., Luo, Zh.-Y., 2013b. Kolosjoki Sedimentary Formation: FAR-DEEP Holes 8A and 8B and related outcrops, in: Melezhik, V.A., Prave, A.R., Fallick, A.E., Hanski, E.J., Lepland, A., R. Kump, L.R. Strauss, H. (Eds.), Reading the Archive of Earth's Oxygenation, Volume 2: The Core Archive of the Fennoscandian Arctic Russia – Drilling Early Earth Project. Springer-Verlag, Berlin-Heidelberg.

Chapter 6.2.5, pp. 693–757.

Melezhik, V.A., Sturt, B.A., 1994. General geology and evolutionary history of the early Proterozoic Polmak-Pasvik-Pechenga-Imandra/Varzuga-Ust'Ponoy Greenstone Belt in the north-eastern Baltic Shield. Earth-Science Reviews 36, 205–241.

Melezhik, V.A., Sturt, B.A., Mokrousov, V.A., Ramsay, D.M., Nilsson, L.-P., Balashov, Yu.A., 1994. The early Proterozoic Pasvik-Pechenga Greenstone Belt: 1:200,000 geological map, stratigraphic correlation and revision of stratigraphic nomenclature. Norges Geologiske Undersøkelse, Special Publication 7, 81–91.

Ohmoto, H., Watanabe, Y., Yamaguchi, K. E., Naraoka, H., Haruna, M., Kakegawa, T., 2006. Chemical and biological evolution of early Earth: constraints from banded iron formations. Geological Society of America, Memoir 198, 291–331.

O'Leary, M.H., 1981. Carbon isotope fractionation in plants. Phytochemistry 20, 553–567.

Papineau, D., 2010. Global biogeochemical changes at both ends of the Proterozoic: insights from phosphorites. Astrobiology 10, 165–181.

Pavlov, A.A., Kasting, J..F., 2002. Mass-independent fractionation of sulfur isotopes in Archean sediments: Strong evidence for an anoxic Archean atmosphere. Astrobiology 2, 27–41.

Pedley, H.M., Rogerson, M., 2010. Introduction to tufas and speleothems, in: Pedley, H.M., Rogerson, M. (Eds.), Tufas and Speleothems: Unravelling the Microbial and Physical Controls. Geological Society, London, Special Publication 336, pp. 1–5.

Pentecost, A., 2005. Travertine. Springer–Verlag, Berlin. 446 pp.

Pentecost, A., Viles, H., 1994. A review and reassessment of travertine classification. Géographie Physique et Quaternaire 48, 305–314.

Pickard, A.L., 2003. SHRIMP U-Pb zircon ages for the Palaeoproterozoic Kuruman Iron Formation, Northern Cape Province, South Africa: evidence for simultaneous BIF deposition on Kaapvaal and Pilbara cratons. Precambrian Research 125, 275–315.

Petrov, V.P., Voloshina, I.M., 1995. Regional metamorphism of the Pechenga area rocks, in: Mitrofanov, F.P and Smol´kin, V.F. (Eds), Magmatism, Sedimentogenesis and Geodynamics of the Pechenga Paleorift. Apatity: Kola Science Centre, pp. 164 - 82. (In Russian)

Pokrovskii, B.G., Melezhik V.A., 1995. Carbon and Oxygen Isotopic Variations in the Lower Proterozoic Carbonates of the Kola Peninsula. Stratigraphy and Geological Correlation 3, 461-472. (Translated from Straigrafiya. Geologischeskaya Korrelyatsiya, Vol 3, No. 5, 42–53)

Préat, A., Bouton, P., Thiéblemont, D., Prian, J-P., Ndounze, S.S., Delpomdor, F., 2011. Paleoproterozoic high $\delta^{13}C$ dolomites from the Lastoursville and Franceville basins (SE Gabon): Stratigraphic and synsedimentary subsidence implications. Precambrian Research 189, 212-228.

Rainey, D.K., Jones, B., 2009. Abiotic versus biotic controls on the development of the Fairmont Hot Springs carbonate deposit, British Columbia, Canada. Sedimentology 56, 1832–1857.

Rasmussen, B., Buick, R., 1999. Redox state of the Archean atmosphere: evidence from detrital heavy mineral in ca. 3250 – 270 Ma sandstones from Pilbara Craton, Australia. Geology 27, 115–118.

Renaut, R.W., Jones, B., 1997. Controls on aragonite and calcite precipitation in hot springs travertines at Chemurkeu, Lake Bogoria, Kenya. Canadian Journal of Earth Sciences 34, 801–818.

Reuschel, M., Melezhik, V.A., Whitehouse, M.J., Lepland, A., Fallick, A.E., Strauss, H., 2012. Isotopic evidence for a sizeable seawater sulfate reservoir at 2.1 Ga. Precambrian Research 192–195, 78–88.

Salminen, P.E., Melezhik, V.A., Hanski, E.J., Lepland, A., Romashkin, A.E., Rychanchik, D.V., Luo, Zh.-Y., Sharkov, E.V., Bogina, M.M., 2013. Kuetsjärvi Sedimentary Formation: FAR-DEEP Hole 5A, Neighbouring Quarry and Related Outcrops, in: Melezhik, V.A., Prave, A.R., Fallick, A.E., Hanski, E.J., Lepland, A., R. Kump, L.R. Strauss, H. (Eds.), Reading the Archive of Earth's Oxygenation, Volume 2: The Core Archive of the Fennoscandian Arctic Russia – Drilling Early Earth Project. Springer-Verlag, Berlin-Heidelberg. Chapter 6.2.2, pp. 617–649.

Schidlowski, M., Eichmann, R., Junge, C.E., 1975. Precambrian sedimentary carbonates: carbon and oxygen isotope geochemistry and implications for the terrestrial oxygen budget. Precambrian Research 2, 1–69.

Schidlowski, M., Eichmann, R., Junge, C.E., 1976. Carbon isotope geochemistry of the Precambrian Lomagundi carbonate province, Rhodesia. Geochimica et Cosmochimica Acta 40, 449–455.

Schidlowski, M., Hayes, J.M., and Kaplan, I.R., 1983. Isotopic inferences of ancient biochemistries: Carbon, sulfur, hydrogen and nitrogen, in Schopf, J.W. (Ed.), Earth's earliest biosphere — Its origin and evolution. Princeton University Press, Princeton, New Jersey, p. 149–186.

Scholle, P.A., Arthur, M.A., 1980. Carbon isotope fluctuations in Cretaceous pelagic limestones: Potential stratigraphic and petroleum exploration tool. The American Association of Petroleum Geologist Bulletin 64, 67–87.

Schröder, S., Bekker, A., Beukes, N.J., Strauss, H., van Niekerk, H.S., 2008. Rise in seawater sulphate concentration associated with the Paleoproterozoic positive carbon isotope excursion: evidence from

sulphate evaporites in the 2.2–2.1 Gyr shallow-marine Lucknow Formation, South Africa. Terra Nova 28, 108–117.

Scott, C., Lyons, T. W., Bekker, A., Shen, Y., Poulton, S. W., Chu, X., Anbar, A.D., 2008. Tracing the stepwise oxygenation of the Proterozoic ocean. Nature, 452, 456–459.

Sial, A., Karhu, J.A., Ferreira, V.P., 2010. Insights from isotope stratigraphy. Precambrian Research 182, v–ix.

Sreenivas, B., Das Sharma, S., Kumar, B., Patil, D.J., Roy, A.B., Srinivasan, R., 2001. Positive $\delta^{13}C$ excursion in carbonate and organic fractions from the Paleoproterozoic Aravalli Supergroup, Northwestern India. Precambrian Research 106, 277–290.

Stiller, M., Rounick, J.S., Shasha, S., 1985. Extreme carbon-isotope enrichments in evaporitic brines. Nature 316, 434–435.

Summons, R.E., Hayes, J.M., 1992. Principles of molecular and isotopic biogeochemistry, in: Schopf, J.W., Klein, C. (Eds.), The Proterozoic Biosphere. Cambridge University Press, Cambridge, pp. 83–93.

Tang, H., Chen, Y., Wu, G., Lai, Y., 2011. Paleoproterozoic positive $\delta^{13}C_{carb}$ excursion in the northeastern Sino-Korean craton: evidence of the Lomagundi Event. Gondwana Research 19, 471–481.

Usdowski, E., Hoefs, J., Menschel, G., 1979. Relationship between ^{13}C and ^{18}O fractionation and changes in major element composition in a Recent calcite-depositing springs—a model of chemical variations with inorganic $CaCO_3$ precipitation. Earth and Planetary Science Letters 42, 267–276.

Valley, J.W., 1986. Stable isotope geochemistry of metamorphic rocks, in: Valley, J.W., Taylor, H.P., O'Neil, J.R. (Eds.), Stable Isotopes in High Temperature Geological Processes. Reviews in Mineralogy, Volume 16, Mineralogical Society of America, pp. 445–489.

Veizer, J., 1983. Chemical diagenesis of carbonates: theory and application of the trace element technique, in: Arthur, M.A., Anderson, T.F., Kaplan, I.R., Veizer, J., Land, L.S. (Eds.), Stable Isotope in Sedimentary Geology. SEPM Short Course No. 10. Chapter 3. Dallas.

Veizer, J., Clayton, R.N., Hinton, R.W., 1992. Geochemistry of Precambrian carbonates: IV. Early Paleoproterozoic (2.25 + 0.25 Ga) seawater. Geochimica et Cosmochimica Acta 56, 875–885.

Wigley, T.M.L., 1973a. Chemical evolution of the system calcite–gypsum–water. Canadian Journal of Earth Sciences 10, 306–314.

Wigley, T.M.L., 1973b. The incongruent solution of dolomite. Geochimica et Cosmochimica Acta 37, 1397–1402.

Yudovich, Y.E., Makarikhin, V.V., Medvedev, P.V., Sukhanov, N.V., 1991. Carbon-isotope anomalies in carbonates of the Karelian Complex. Geochemistry International 28, 56–62.

Yoshimura, K., Liu, Z., Cao, J., Yuan, D., Inokura, Y., Noto, M., 2004 Deep source CO_2 in natural waters and its role in extensive tufa deposition in the Huanglong Ravines, Sichuan, China. Chemical Geology 205, 141–53.

Young, G.M., Long, D.G.F., Fedo, C.M., Nesbitt, H.W., 2001. Paleoproterozoic Huronian basin; product of a Wilson cycle punctuated by glaciations and a meteorite impact. Sedimentary Geology 141–142, 233–254.

Zagnitko, V.N., Lugovaya, I.P., 1989. Isotope Geochemistry of Carbonate and Banded Iron Formations of the Ukrainian Shield. Naukova Dumka, Kiev (in Russian).